AD NUMBER

AD426840

NEW LIMITATION CHANGE

TO

Approved for public release, distribution unlimited

FROM

No Foreign

AUTHORITY

DNA ltr., 29 May 1973

WT-1152

Copy No.

1115787

Operation TEAPOT

NEVADA TEST SITE

February – May 1955

Project 9.4

ATOMIC CLOUD GROWTH STUDY

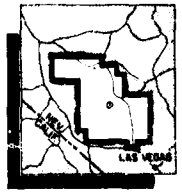

HEADQUARTERS FIELD COMMAND, ARMED FORCES SPECIAL WEAPONS PROJECT
SANDIA BASE, ALBUQUERQUE, NEW MEXICO

[redacted]

WT-1152

This document consists of 138 pages

No. 202 of 240 copies, Series A

[redacted]

OPERATION TEAPOT

Project 9.4

ATOMIC CLOUD GROWTH STUDY

~~Report to the Test Director~~

by

B. A. Grossman
L. Machta
L. R. Quenneville
S. W. Dossi
J. Halsey

October 1955

[redacted]

Air Force Cambridge Research Center
Boston, Massachusetts

[redacted]

SUMMARY SHOT DATA

SHOT	CODE NAME	DATE	TIME *	AREA	TYPE	LATITUDE & LONGITUDE OF GROUND ZERO
1	Wasp	18 February	1200	T-7-4 1/	762' Air	37° 05' 18.6856" 116° 01' 18.7366"
2	Moth	22 February	0545	T-3	300' Tower	37° 02' 52.2654" 116° 01' 15.1967"
3	Tesla	1 March	0530	T-9b	300' Tower	37° 07' 31.5737" 116° 02' 51.0077"
4	Turk	7 March	0520	T-2	500' Tower	37° 08' 18.4944" 116° 07' 03.1679"
5	Hornet	12 March	0520	T-3a	300' Tower	37° 02' 25.4043" 116° 01' 31.3674"
6	Bee	22 March	0505	T-7-1a	500' Tower	37° 05' 41.3880" 116° 01' 25.5474"
7	ESS	23 March	1230	T-10a	67' underground	37° 10' 06.1263" 116° 02' 37.7010"
8	Apple	29 March	0455	T-4	500' Tower	37° 05' 43.9200" 116° 06' 09.9040"
9	Wasp'	29 March	1000	T-7-4 3/	740' Air	37° 05' 18.6856" 116° 01' 18.7366"
10	HA	6 April	1000	T-5 3/	36620' MSL Air	37° 01' 43.3642" 116° 03' 28.2624"
11	Post	9 April	0430	T-9c	300' Tower	37° 07' 19.6965" 116° 02' 03.8850"
12	MET	15 April	1115	FF	400' Tower	36° 47' 52.6887" 115° 55' 48.1086"
13	Apple 2	5 May	0510	T-1	500' Tower	36° 03' 11.1095" 116° 06' 09.4937"
14	Zucchini	15 May	0500	T-7-1a	500' Tower	37° 05' 41.3880" 116° 01' 25.5474"

* APPROXIMATE LOCAL TIME - PST PRIOR TO 24 APRIL, PDT AFTER 24 APRIL
1/ ACTUAL GROUND ZERO 36' NORTH, 426' WEST OF T-7-4
2/ ACTUAL GROUND ZERO 94' NORTH, 62' WEST OF T-7-4
3/ ACTUAL GROUND ZERO 36' SOUTH, 397' WEST OF T-5

ABSTRACT

The purpose of this project was twofold: first, to document the evolution of atomic clouds during the TEAPOT series in order to define the rate of rise, maximum height, vertical depth of mushroom, dimensions of stem and volume, for a period up to 20 min after burst when photographically feasible; second, to correlate the meteorological data with the available cloud data on past Nevada test series as well as the TEAPOT series. Operating commands, in particular the Strategic Air Command and the Air Defense Command, have indicated a need for such information relative to offensive and defensive tactics.

Photographic data were collected and analyzed by Edgerton, Germeshausen & Grier. Army Map Service participated in Shots 10, 11, and 12 to check out a photographic method of cloud volume determination by a stereoscopic procedure. The U. S. Weather Bureau and Air Force Cambridge Research Center effected the correlation of cloud data with atmospheric parameters and made theodolite observations of cloud rise and height on each shot. Strategic Air Command (Project 40.5) photographed the rising cloud from directly above the burst at short time increments after H-hr.

Photographic and theodolite data were collected on 14 shots. Analysis of weather parameters affecting cloud heights attained does not suggest any clear-cut definitions with the exception of the tropopause dampening effect. Application of current theories has been investigated and the results compared.

Army Map Service volume analysis was not feasible on the high altitude shot because of lack of density of the smoke ring. Volume analysis was not feasible on Shot 11 (predawn) because of lack of light. On Shot 12 nonsynchronization of photo pairs did not permit a feasibility evaluation.

FOREWORD

This is one of the reports presenting the results of the 47 projects participating in the Military Effects Tests Program of Operation TEAPOT, which included 14 test detonations. For readers interested in other pertinent test information, reference is made to WT-1153, Summary Report of the Technical Director, Military Effects Program. This summary report includes the following information of possible general interest.

a. An over-all description of each detonation, including yield, height of burst, ground zero location, time of detonation, ambient atmospheric conditions at detonation, etc., for the 14 shots.
b. Discussion of all project results.
c. A summary of each project, including objectives and results.
d. A complete listing of all reports covering the Military Effects Tests Program.

ACKNOWLEDGMENTS

The general cooperation and helpfulness of the Directorate of Weapons Effects Tests group was worthy of note. In particular, appreciation should be expressed to the following personnel:

Lt Col Jack G. James and Maj William M. Sheahan, Program 9 Director and Assistant Director, respectively, for their assistance and support during the TEAPOT series.

Lt Col Clifford Spohr, Lt Col Ralph Steele, and Maj Robert McKown, Air Weather Service officers, for making available the necessary weather information and permitting the use of the theodolite for cloud measurements.

Col Paul Fackler, Lt Col Frank Carlson, Maj Jack DeVries, and Maj F. A. Mitchell of the Air Force Special Weapons Center for their cooperation in gathering cloud information from sampling aircraft.

Capt C. S. Adler, Directorate of Weapons Effects Tests, for assistance in arranging timing signals.

Mr. Kenneth M. Nagler, U. S. Weather Bureau, for assistance with the theodolite measurements and computations.

Mr. D. Bucci and Capt D. Henderson, Army Map Service, who conducted their field camera operations at the Nevada Test Site.

The extensive drafting and typing assistance of the Reports Branch of the Military Effects Group is also gratefully acknowledged.

CONTENTS

ILLUSTRATIONS

TABLES

CHAPTER 1

INTRODUCTION

1.1 OBJECTIVE

The objective of the overall project was to accumulate complete and accurate cloud data and correlate these data with yield, height of burst, and meteorological information in order to derive general rules relative to the evolution of an atomic cloud. Operating commands, in particular the Strategic Air Command (SAC) and the Air Defense Command (ADC), have indicated a need for such information relative to offensive and defensive tactics.

1.2 BACKGROUND

1.2.1 Past Cloud Measurements, History

According to available reports, initial collection of atomic cloud rise and height data was accomplished at the SANDSTONE tests (April, 1948) by means of manually controlled theodolites. 1/ This project was organized by the Task Group with the cooperation of the Air Force, Navy, and Weather Bureau.

During the RANGER series (Jan-Feb, 1951) the Air Weather Service (AWS) made additional theodolite measurements documenting cloud rise and height. 2/

In April, 1951, during the GREENHOUSE series, cameras were first utilized to accumulate cloud information, and a theoretical study was completed by Kellogg, et al. 3/

During the BUSTER-JANGLE series (Oct-Nov, 1951) further theodolite measurements were completed by the AWS 4/, and Edgerton Germeshausen & Grier (EG&G) used camera equipment for cloud documentation from stations less than 10 miles from burst point.

During the TUMBLER-SNAPPER series (April-May, 1952) the AWS again made cloud measurements by means of theodolites. 5/ Because of the low priority to cloud information, photographs by EG&G were taken only for 30 sec, primarily for an Atomic Energy Commission (AEC) interest rather than total cloud evolution.

In November, 1952, at the IVY series, EG&G utilized cameras based on land, ships, and aircraft to document the cloud history. 6/,7/

During the UPSHOT-KNOTHOLE tests (Mar-Jun, 1953) both the AWS with theodolites 6/ and EG&G by means of camera stations, 7/ documented the cloud growth.

On the CASTLE series (Mar-May, 1954) EG&G again used land-, sea-, and air-based cameras to obtain photographic cloud data. 10/

1.2.2 Past Cloud Measurements, Evaluation

In correlating the existent cloud data, it was believed wise to consider initially the Nevada Test Site (NTS) data exclusively before including the Pacific Proving Grounds' cloud data, the bulk of which is in the megaton yield category. In reviewing the available records of cloud data collected at the Nevada site, it was discouraging to note that only nine shots out of greater than 30 detonations offered cloud rise and height data which could be considered reliable. The definition "reliable" would depend upon the applicability of the data for a correlation study of effects of yield, height of burst, and meteorological parameters on the cloud evolution. The major reasons for the paucity of data were as follows: (1) single camera station data did not offer sufficient reliability, primarily due to no drift correction when the cloud vectored toward the camera; (2) theodolite data did not afford sufficient accuracy because of manual operation; and (3) when both the camera and theodolite data were available, in some cases, there were large differences in data values.

In report AFSWP 501, the linear relationship of the cloud height vs log yield is presented for all shots prior to the spring 1953 series. 13/ After adding UPSHOT-KNOTHOLE data based upon AWS and EG&G records, the standard error from the above curve was 4300 ft.

Thus, it was apparent that thorough and accurate cloud data were required to permit a careful analysis of the importance of meteorological effects and initial conditions on cloud evolution.

1.3 THEORY

1.3.1 General Considerations

The evolution of the stabilized atomic cloud, while smaller, must obey the physical laws governing the heat loss and atmospheric processes which determine the history of a heated bubble of air. In particular, it is likely that the main reduction in temperature in the fireball stages results from radiative loss and that the atmosphere plays essentially no role during these early periods. The atmosphere becomes important in reducing the mean temperature of the cloud in three ways: first, in producing an expansion of the atomic cloud as it rises; second, in providing cooler air to entrain into the atomic cloud, and third, in determining the rate at which the atmosphere reduces its buoyancy. The decrease of pressure with height is almost the same for all atmospheres and, at present, it is felt that the cloud, rather than the atmosphere, determines how much air is being entrained. It is only in respect to the third item (which is essentially the atmosphere's lapse rate of temperature) that there is a real variation from shot to shot. The probable

control of the atmosphere over the maximum rise of the atomic cloud through the lapse rate is illustrated by large numbers of clouds which stop at the tropopause, by the several low-yield shots which stopped at inversions in the troposphere, and by the horizontal layers of the stem material below stable layers.

The discussion mentioned above is, strictly speaking, applicable to a dry atmosphere. The moisture (in vapor state) entrained in the lower levels is of the order of 1 to 10 grams per kilogram of air which condenses at the lower temperatures of the upper atmosphere to release about 600 calories of heat for each gram of water vapor. For Nevada shots the releases of this amount of heat probably does not exceed an additional 0.1 KT of energy, but, in the case of Pacific shots where the moisture content of the air is much higher, this may be much more important.

In describing the evolution of an atomic cloud there are many features which are of interest. Among these are: the absolute top of the cloud, the top of the body of the cloud, the center of gravity of the mushroom, the base of the mushroom, the bases and tops of layers (if any) of the stem, the width of the mushroom and stem, the volume of the mushroom and stem, and the delineation of the radioactivity within the visible cloud. Unfortunately, only the top of the cloud has been systematically observed during each of the tests. The other items have been investigated during only a limited number of the shots. Consequently, theories have been promulgated and tested on the maximum rise of the cloud only.

Two reasonable approaches to the prediction of cloud heights are: first, one can develop formulae which purport to express the physical processes involved in the rise; and second one may compute regression equations in which certain meteorological [illegible]ervation features are the independent variables.

1.3.2 Current Theories

Two ways in which one might predict the maximum rise of the cloud are: First, one might attempt to determine the elevation at which the cloud and environment are at the same temperature plus assuming a negligible amount of "overshooting" of the level of no further buoyancy; second, one might assume that the cloud height attained is equal to the computed upward motion. While the latter approach appears to be far more reasonable, it requires a knowledge of the resistance of the atmosphere to the upward motion of the cloud mass, a feature which is known very imperfectly.

There are in existence three published theories of the maximum rise of the cloud, two of which yield similar results.

(1) Taylor [17] has suggested a theory in which the rate of entrainment of air into the surface of the cloud is represented by αu, where α is the entrainment factor and u is the upward speed of the cloud. Siddons [19] showed how the resistance of the air could be incorporated with Taylor's formulation of the rise of a heated bubble.

(2) Sutton [18] prepared a theory of the rise of a cloud based on his diffusion theory.

(3) Machta 11/ devised a formula of the maximum height assuming that the percentage rate of entrainment per unit height is a constant over a given height interval.

All of the theories incorporate the effects of the expansion of the cloud as it rises through the use of the potential rather than the actual temperature.

Table 1.1 gives the formulae of Taylor, Sutton, and Machta for the maximum rise of a heated bubble through the atmosphere. Column I gives the formula for the height at which the cloud is no longer buoyant, whereas Column II provides the height at which the upward velocity ceases.

It should be noted that only the Taylor resistance equation in Column II incorporates the resistance of the air to the rising cloud. The Sutton and Machta* formulae do not. Further, the value of C_D used in Taylor's formula must be admitted to be quite uncertain.

It is possible to compute the height of the cloud in stepwise fashion to eliminate the need to keep such quantities as the density constant through a great depth of the atmosphere.

All of the formulae suffer from a lack of knowledge of the residual energy of the explosion which provides the heat for the buoyancy. The Taylor and Sutton formulae already have converted this energy into a temperature rise which has not been done in the Machta formula. In each of the formulae there is one main quantity which determines the rise. This is the entrainment: α in the case of Taylor's formula, C in the case of Sutton's and $\partial M/M\partial z$ in the case of Machta's. In each formula this quantity dominates all others, and in each case, it is felt, the applicable value is probably known with great uncertainty. Each formula derives its entrainment rate from other measurements of atmospheric phenomena and the authors show that each of the resulting answers is not unreasonable. It might also be pointed out that the exponent in the Sutton equation for reasonable values of the pertinent parameters is about the same as that in Taylor's equation.

One should expect the heights achieved by the formulae in Column II to be appreciably greater than those in Column I, since the cloud still has an upward velocity when it no longer is lighter than the environment. While it must be true that the cloud "overshoots" the level of no buoyancy, the magnitude of such overshooting is not felt to be from 20,000 to 54,000 ft as one computation of the two Taylor equations indicate. In Nevada, the sinking of the cloud within the first 15 minutes after initial stabilization rarely exceeds 5000 ft and part of the subsidence of the top may be due to factors other than the overshooting (e.g., sinking of particles, descending atmospheric motion, etc.).

Certain general conclusions can be derived from all of the formulae:

(1) The cloud rise is sensitive to the entrainment and is less sensitive to the energy yield of the device or temperature excess of the fireball.

* The maximum rise of the cloud using the level of no further motion was not promulgated by Machta nor Sutton but is given in Ref. 17.

(2) The main defect in the use of motion, rather than the level of no buoyancy as the measure of maximum height, lies with the lack of knowledge of the resisting action of the atmosphere. The height predicted by the formulae at which there are no longer any buoyancy effects is too low, but whether this is a thousand feet or so as the present authors believe, or 24,000 ft as deduced by Cohen, [20] is still unproved.

(3) The formulae would more correctly predict the height of the center of the mushroom rather than the tops, even though many of the verifications have been applied to the cloud tops since these were all that were available.

TABLE 1.1 - Application of Theory of Cloud Evolution by Taylor, Sutton, and Machta

	Column I (Buoyancy)	Column II (Vertical Velocity)
Taylor	$H = \left[\frac{3E}{\pi\rho\sigma\beta a^3}\right]^{1/4}$	$H = \left[\frac{6E}{\pi\rho\sigma\beta a^3}\right]^{1/4}$
Taylor-resistance		$H = \left[\frac{3E(7 + C_D/2\alpha}{\pi\rho\sigma\beta a^3(3+C_D/2\alpha)}\right]^{1/4}$
Sutton	$H = \left[\frac{(3m + 2p)E}{4\pi^{3/2}\rho\sigma G^3\beta_p}\right]^{2/(3m+2p)}$	$H = \left[\frac{2E(3m+2p)(3m+p+1)}{9\pi\rho\sigma G^3\beta(3m+2)p}\right]^{2/(3m+2p)}$
Machta	$H = \frac{1}{\frac{1}{N}\frac{\partial N}{\partial z}} \log_e\left[1 + \frac{\frac{1}{N}\frac{\partial N}{\partial z}\Delta\theta_o}{\beta}\right]$	Solution of Equation: $\left[u(o)\right]^2 + 2g\int_o^H \left(\frac{\Delta\theta_e}{\theta_o} - \frac{2}{N}\frac{\partial N}{\partial z}\right) z \, dz = o$

Where H = height of cloud above level at which fireball radiation effects become negligible
E = heat energy available to raise the temperature of the cloud for buoyancy
g = acceleration due to gravity
ρ = density of cloud (a mean value along the cloud ascent)
β = potential temperature lapse rate of the air
α = entrainment rate of Taylor's theory (0.2)
C_D = drag coefficient (suggested value in range 0.5 to 1.0
m = a stability factor in Sutton's diffusion theory (suggested value = 7/4)
σ = specific heat of air at constant pressure (0.25 cal/gm/°K)
p = exponent in a formula for potential temperature gradient which is of the form zP (normally p = 1)

$(1/M)(\partial M/\partial z)$ = percentage rate of mass M entrainment per unit height z, a constant

$\Delta\theta_o$ = potential temperature excess of cloud over environment at time when radiation effects are negligible

$u(o)$ = upward speed at the level at which the radiation no longer is important

θ_o = potential temperature at level at which radiation effects are negligible

To solve the integral in Column II, use

$$\Delta\theta = \left[\Delta\theta_o + \frac{\beta}{\frac{1}{M}\frac{\partial M}{\partial z}}\right] e^{-\frac{1}{M}\frac{\partial M}{\partial z}} - \frac{\beta}{\frac{1}{M}\frac{\partial M}{\partial z}}$$

1.3.3 Empirical Formulae

If one has many cases of the rise of clouds under different weather conditions, one may select the most likely feature of the atmosphere and the physical parameters which determine the maximum rise of the cloud and empirically determine a formula which predicts the rise. The AWS group at Los Alamos Scientific Laboratory (LASL) has done this with the following results as of the present.

For 1 to 10 KT shots both tower and air bursts*

$$Y = 17 + 2.16x_1 - 5.43x_2 + 0.34x_3$$

where Y = amount of rise of cloud (1000's of ft)
x_1 = yield in kilotons
x_2 = departure (in °C) of actual lapse rate from the adiabatic lapse rate (mean of 50-mb increments) from 850 mbs to cloud top
x_3 = mean wind in knots in layer through which cloud rises

For air bursts (10 to 60 KT)

$$Y = 29.73 - 0.1098x_1 - 0.072x_2 - 1.7681x_3 + 2.1863x_4 - 0.4852x_5$$

For 300-ft tower bursts (10 to 50 KT)

$$Y = 31.9436 + 0.0202x_1 - 0.0849x_2 - 5.3230x_3 + 0.5767x_4$$

where Y = maximum height (1000's of ft above MSL)
x_1 = yield in kilotons
x_2 = mean wind in knots from 10,000 to 35,000 ft in 5000-ft increments

* Newgarden and Spohn, LASL, unpublished.

x_3 = departure (in °C) of actual lapse rate from the adiabatic lapse rate (mean of 50-mb increments) from 600 to 400 mbs
x_4 = height of tropopause (1000's of ft above MSL)
x_5 = height of burst (1000's of ft above ground)

The defects in the use of empirical formulae are twofold: first the parameters which are used in the regression equation, while probably applicable, may not necessarily affect the height in a linear relationship, and second, the regression equations use only the easily determined meteorological parameters rather than such terms as entrainment or superheat, directly related to theoretical endeavors to solve the cloud rise problem.

In the present state of atomic cloud-top predictions, there is a definite place for regression equations, but they should be used with caution and modified when contradictory to the sense of the theory.

1.3.4 Past Data vs Theory

Data concerning cloud evolution collected through the spring of 1953, at Nevada, do not appear to support the theory except when viewed in a broad picture. It is to be expected that, since meteorological conditions are selected at random with respect to cloud evolution, one ought to find a clear increase in cloud height with yield. Secondly, there should be a predominance of clouds which stop slightly above the tropopause, since the stratospheric stability should inhibit further rise.

Prior observations do, in fact, show that devices with yields over approximately 15 KT rise appreciably higher than those below approximately 15 KT. Figure 1.1 indicates past cloud rises compared to yield. In the lower range, up to 15 KT, the theory is qualitatively verified by a general increase in cloud rises with yield. However, above about 15 KT (and up to about 60 KT) the data suggest that the amount of rise of the cloud top is almost independent of the yield of the device. In fact, the amount of rise in this yield range appears to be uncorrelated to anything thus far studied. This condition resulted in the curious fact that the use of a fixed altitude (i.e., average height of tropopause) as the stopping point for UPSHOT-KNOTHOLE clouds in the 15 to 60 KT range was superior to the existing regression equations prepared from pre-UPSHOT-KNOTHOLE information.

Study of the relationship between the tropopause and the maximum rise of the cloud in this range of yields improved the situation only slightly. Above about 40 KT all cloud tops entered the stratosphere by the same amount, while below 40 KT the stratospheric penetration failed to correlate with yield.

It is felt that there probably does exist some significant control by the atmosphere on the maximum height of the clouds accounting in part for their differences. A review of the probable reasons for failure to detect any such control suggests the poor quality of the cloud evolution observations as the cause.

1.3.5 Special Case

One of the most interesting shots of the TEAPOT series, relative to atomic cloud growth, was the 36,600 ± 300-ft burst of a small KT weapon.

Since it was anticipated that the burst height would place the weapon in the stratosphere rather than the troposphere, two new conditions were now introduced: (1) air density was lower by a factor of 4 compared to surface conditions; and (2) the atmospheric lapse rate became almost isothermal, resulting in far greater stability.

Primarily because of the sampling problem, much interest was directed to the anticipated maximum cloud height. Meteorologically, the problem was fascinating because of the new environment of the stratosphere in which the atomic cloud would evolve.

Kellogg of the Rand Corporation, at the request of Air Force Cambridge Research Center (AFCRC), considered this problem. 12/ An assumption was made that the fireball radius is inversely proportional to the air density. In this case, greater heat would be used up initially to heat the greater mass of air and the initial vertical acceleration would decrease. In addition, the previously mentioned Machta equation (Table 1.1, Column I) was utilized. The entrainment factor M/M_z is relatively insensitive to yield and can be given a numerical value of 2×10^{-3} to 3×10^{-3}. The stability term (β) is well known in the stratosphere and equals $10 \times 10^{-3} m^{-1}$. The possible range of initial superheat $(\Delta\theta)_o$ is quite large and probably varies between 600°K to 2000°K. By further simplification of the above equation, a ratio is set up comparing tropospheric with stratospheric terms. The results suggest that the cloud would rise 0.80 to 0.88 as high at 40,000 ft as compared to near surface detonations. This result suggests that a 2 KT bomb burst at 40,000 ft would rise to 48,000 ft (center of cloud).

Another similar effort to solve this problem resulted in a meeting at the AFCRC in June, 1954, attended by the U. S. Weather Bureau and AWS representatives. Consideration was given to the Sutton and Taylor formulae in Table 1.1 using as a reasonable approximation

$$h \approx \left[\frac{1}{\rho\beta}\right]^{0.25}$$

In comparing the heights to be attained in the troposphere and stratosphere, the yield term E can be neglected since it remains constant. By inserting numbers for the other terms involved, the ratio becomes 0.88, quite similar to the Kellogg approximation. This again suggested that the high altitude burst would not rise as far vertically as its lower counterpart.

The above estimates are based primarily on the effect which the stability and density of the atmosphere will have on the rising bubble which is given a fixed amount of heat energy. However, according to Kellogg, 21/ the dimensions of atomic clouds detonated at different pressures should be corrected for the work which the fireball must do

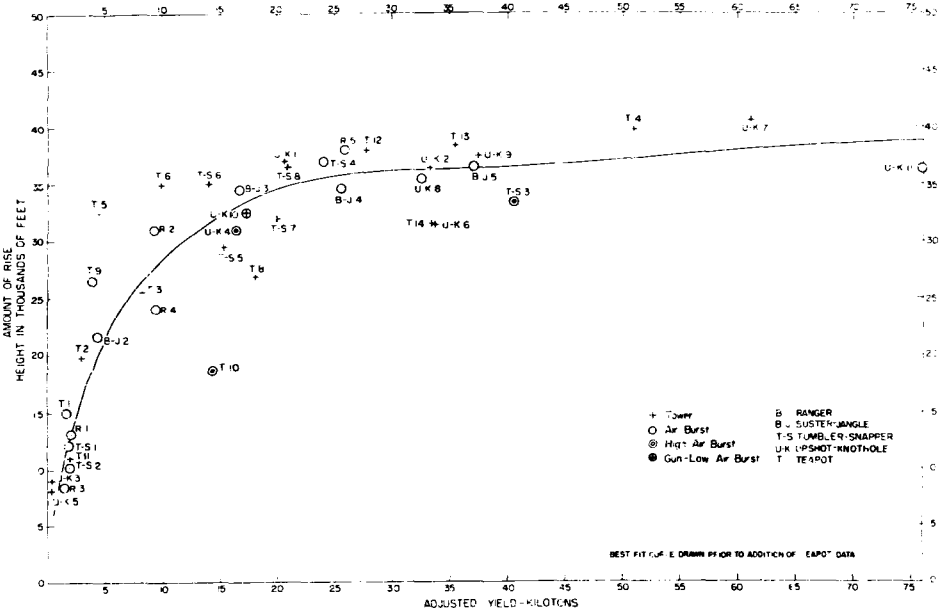

Fig. 1.1 Past Data Yield vs Height

in expanding against the environment. This correction is inversely proportional to the pressure at detonation level. If the high air burst is exploded at about 40,000 ft (or about 200 millibars) and is to be compared with tower or low-level bursts in Nevada at a height of about 4500 ft (or about 860 millibars) then the ratio 860/200, or about 4 should be applied. This correction was not envisaged when planning estimates of the high air burst rise were prepared and comparisons between observed and calculated heights in this report are based on its omission.

CHAPTER 2

EXPERIMENTAL PROCEDURE

2.1 EDGERTON, GERMESHAUSEN & GRIER PARTICIPATION

Edgerton, Germeshausen & Grier photographed the atomic cloud on each detonation in order to determine the following parameters: cloud height, rate of rise, vertical depth of mushroom, dimensions of stem, and volume.

2.1.1 Instrumentation and Equipment

One Bell and Howell 35 mm Two 70 mm cameras *One A/6 35 mm	Station 9.4a at Charleston Peak and Station 9.4b at Amargosa
One Bell and Howell 35 mm *One A/6 35 mm	Station 372 near Control Point (CP)

*Discontinued after first shot because of unreliability

2.1.2 Location of Camera Sites

	Latitude	Longitude	Approximate Location
Station 9.4a - Charleston Peak	36°-19.1'	115°-34.5'	43 miles SE of CP
Station 9.4b - Amargosa	36°-23.01'	116°-26.31'	50 miles SW of CP
Station 372 - near CP	36°-56.2'	116°-04.2'	1 mile W of CP

2.1.3 Operations

Three camera locations were operated by EG&G to accumulate photographic data for Project 9.4.

(1) Station 372 (also collected fireball and cloud data for AEC Projects 15.2 and 23.2). At this station two 35 mm cameras, having focal lengths of 102 and 50 mm respectively, were run at 2.4 and 24 frames per second (fps) for 4 and 10 minutes, respectively. Wide angle lenses were utilized to see as high as possible.

(2) Station 9.4a (Charleston Peak). One A/6 camera, focal length 102 mm, was run at 24 fps for 4 minutes. The Bell and Howell camera, focal length 50 mm, was run 1 fps and 2.4 fps for 10 minutes. Both 70 mm cameras, focal length 105 mm, were run at 1 photograph every 15 seconds for 20-30 minutes.

(3) Station 9.4b (Amargosa) same as station 9.4a.

All stations were radio linked and were manned. Camera timers documented the cloud rise on each frame of the film. Apertures were manually adjusted on the cameras during the cloud evolution to compensate for approaching daylight. On daylight shots, some 16 mm kodachrome film was used as added documentation.

The angle subtended at ground zero by the Charleston Peak and Amargosa stations varied from 55° on Shot 4 to 30° on Shot 12, generally about 60° on the other detonations.

Station 372, near the Control Point, was of value for early cloud rise photography. The Charleston Peak (9.4a) and Amargosa (9.4b) stations were of more value for documenting the latter part of the cloud rise and also for determining horizontal drift of the atomic cloud.

Complete details of cameras, lenses, settings, and film used can be found in EG&G planning report 1177 and post TEAPOT film data sheet catalog, EG&G report LV-193.

2.2 ARMY MAP SERVICE PARTICIPATION

Army Map Service participated in Shots 10, 11, and 12 of this test series to determine the feasibility of measuring cloud volume by photogrammetric procedures. The method applied is a modification of methods used in aerial and terrestrial photogrammetric mapping. A pair of overlapping photographs are obtained from two camera positions. When oriented in a precision photogrammetric instrument (Zeiss Stereoplanigraph) a scaled, visual, three dimensional model of all objects (in this case a section of the cloud) within the overlap area of the photographs is obtained. The instrument provides a method of converting this model to an accurately scaled graphic portrayal, on a two dimensional medium with the third dimension indicated by contour lines.

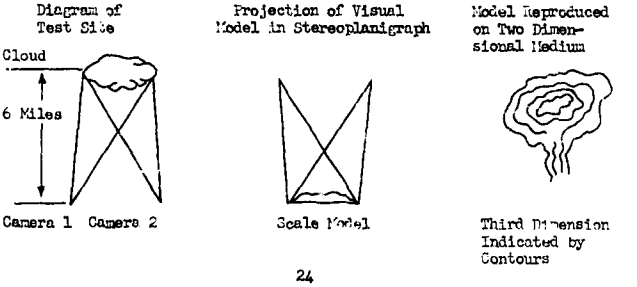

From this diagram of the cloud the volume of the section of the cloud may be computed easily. To determine the complete volume of the cloud, several cameras would have to be placed around the cloud. As this was a feasibility test only, a maximum of three cameras were planned for use on each shot.

2.2.1 Planned, Test Procedure

Initial discussions regarding Army Map Service participation and a general plan of operations were held on 21 September 1954 with representatives of Air Force Cambridge Research Center and the Armed Forces Special Weapons Project. Final plans were prepared by AMS with advice and guidance from AFCRC, including some indication of the AEC safety requirements at the NTS. Studies and experiments were conducted at AMS to determine the camera equipment to be used. The equipment selected by AMS for use was:

3 Type T-11 Aerial Mapping Cameras (selected for uniform operating characteristics)
3 Camera Mounts (manufactured at AMS)
3 Vacuum Pumps (manufactured at AMS)

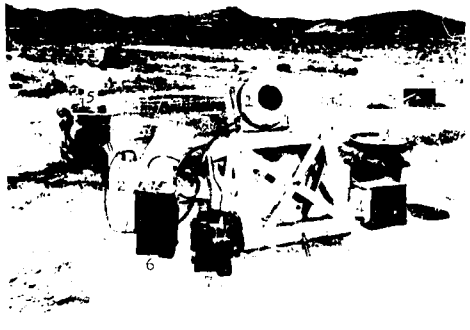

1. T-11 Camera
2. Suction Pump
3. Timer
4. Battery
5. Generator
6. Radio to CP
7. Walkie Talkie

Fig. 2.1 AMS Camera Site

It was agreed, after it was found that AEC had strict limitations on land lines, that EG&G would furnish suitable radio equipment for synchronized triggering of the cameras. The equipment furnished included:

One transmitter (operated by EG&G)
Six Motorola FMRU-1/V, 1-D receivers
Three 110 volt units were used for voice count-down
Three 6 volt units were used for triggering cameras
Three 110 volt generators
Three Two-way, walkie-talkies
Three 6 volt batteries

Three camera station sites were chosen from AMS topographic maps of the NTS for Shot 10 and three for Shot 12. Office selection of stations for Shot 11 was not made as this test was to determine image quality only. Exposures were planned at 5 sec intervals with the first exposure scheduled at zero hour. The cameras would remain in operation until the film supply (200 exposures) was exhausted.

2.2.2 Field Operations

2.2.2.1 Shot 10

The three cameras were installed on the station sites selected. The geographic positions were as follows:

	Latitude	Longitude
Camera 372	36°56.2'	116°04.2'
Camera 1	36°57.4'	115°59.4'
Camera 2	36°57.4'	116°08.5'

After installation, a check of the radio synchronization system was carried out with satisfactory results at all stations. Due to safety requirements only one station was manned during the shot. The radio triggering system failed to activate the camera at this station during the actual shot, possibly due to signal interference, so the camera was operated manually to obtain exposures at approximately 5 sec intervals. It was later determined that one of the two other stations was successfully triggered by radio but no exposures were obtained at the third station.

2.2.2.2 Shot 11

Shot 11 (predawn) was photographed from one manned camera station. The radio signal again failed to trigger the camera so operation was manual. The personnel manning the station observed the light intensity after the shot to judge the possibilities of obtaining a good photo image and found the light very inadequate.

2.2.2.3 Shot 12

The cameras were installed at the selected sites and tested

for radio triggering. No signal was received at two of the three stations so selection of new stations was required. One of the new sites was required by AEC to be unmanned, a double crew was required for the second site and the third site was approved for a single crew. Intermittent signals were received at the stations during a dry run but new stations could not be selected due to lack of time. The radios failed to trigger the cameras during the shot so two cameras were manually operated. The camera locations were:

	Latitude	Longitude
Shot 12 East	36°42'48.5"	115°54'47.2"
Shot 12 West	36°43'05.3"	115°58'14.7"

2.3 STRATEGIC AIR COMMAND PARTICIPATION

As part of the Strategic Air Command's orientation and training program, two B-47's were flown over ground zero, at altitudes of 42,000 ft and 43,000 ft, at 1/2 and 2 min after burst (Project 40.5). Participation occurred on Shots 4, 8, 12, and 13. The purpose of the above flights was to photograph the top of the rising cloud. This information would assist the groups which were analyzing specific parameters. KA 3 cameras, two frames per second, positioned on the belly on a vertical axis were used for the photography. On predawn bursts, the aircraft was flown on a west-east heading to take advantage of any available daylight.

2.4 THEODOLITE MEASUREMENTS

In order to evaluate better the accuracy of past theodolite data, theodolite measurements on rate of rise and maximum cloud height were taken on each shot by U. S. Weather Bureau (USWB) and AFCRC personnel. The theodolite was located at the north fence of the Control Point for all shots, except Shot 10. On Shot 10, the location was on the Frenchman Flat access road so as to provide a longer base line for this high altitude shot. On predawn bursts, in some instances, it was difficult to delineate clearly the cloud during the first minute. In these cases, a clinometer was used to approximate the height attained by the cloud. Correction for wind drift was applied to the theodolite readings to determine actual cloud top. No correction was made for the fact that the actual cloud top was not always being measured, since the edge of cloud obscured the top from the point of observation.

CHAPTER 3

TEST RESULTS

3.1 Shot 1

3.1.1 Edgerton, Germeshausen & Grier Photographic Analysis

Low clouds prevented the use of Amargosa and Angel's Peak camera stations. Station 372 (near the Control Point) data were used to plot Figs. 3.1,* 3.1a, and 3.1b.

3.1.2 Aircraft Reports (See Fig 3.1)

Sampling aircraft, Air Force Special Weapons Center (AFSWC), reported the following cloud data: H + 15 min - top of cloud, 17,500 to 18,000 ft with peaks at 20,000 ft; base of cloud, 14,500 ft.

3.1.3 Theodolite Data

Theodolite Location: Control Point
Horizontal Range: 56,147 ft.
Bearing: 9.7580
Burst Height: 4957 ft MSL

TABLE 3.1 - Theololite Data, Shot 1

Time (min)	Elevation Angle	Horizontal Distance (ft)	Cloud Height (ft MSL)
0.0	-	56,147	4,957
0.5	5.0	56,147	9,055
1.5	8.6	53,500	11,737
2.5	12.5	50,000	15,235
3.0	14.1	48,100	16,146
3.5	15.9	46,100	16,924
4.0	17.4	44,200	18,147
4.5	18.6	42,450	18,000
5.0	19.7	40,800	18,273

* Fig. 3.1 curve is constructed as the best fit curve from computed points not indicated on this chart.

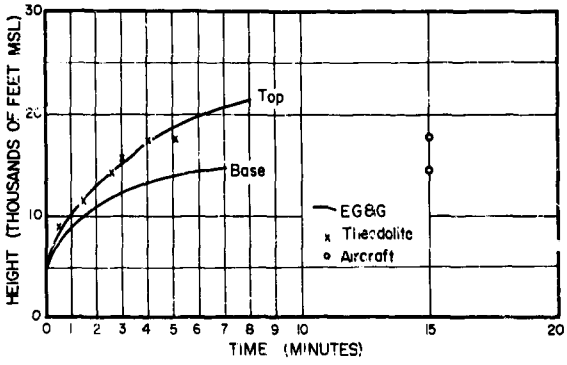

Fig. 3.1 Cloud Rise vs Time, Shot 1

3.1.4 Comparison of Cloud Height Observations

There does not appear to be good agreement on maximum height reached. The fact that the photographic analysis was based upon a single camera station does not justify the usual validity of the photographic analysis.

3.1.5 Weather Data

Clouds: Broken (6/10 - 8/10) 5000 ft
Visibility: 15 mi
Weather: None
Shot Height - (4957 ft MSL): Temperature, -5.5°C; Pressure, 846 mb; Potential Temperature, 281°K
Pseudo-Adiabatic Chart. See Fig. 3.2
Wind Speed and Direction: See Fig. 3.3

3.1.6 Comparison of Cloud and Weather Data

According to past data (Fig. 1.1) the cloud rose a few thousand feet above the expected height. The lapse rate (interpolated) for shot time indicated a relatively unstable layer to 15,000 ft (tending to increase the cloud height) and a strong inversion from about 15,000 to 18,000 ft which should have been effective in slowing down the rise of the cloud. A stable layer above the inversion to 22,000 ft should also have acted to dampen the cloud rise. A consistent wind direction above 10,000 ft and strong vertical wind shear should have acted to decrease the height attained by the cloud.

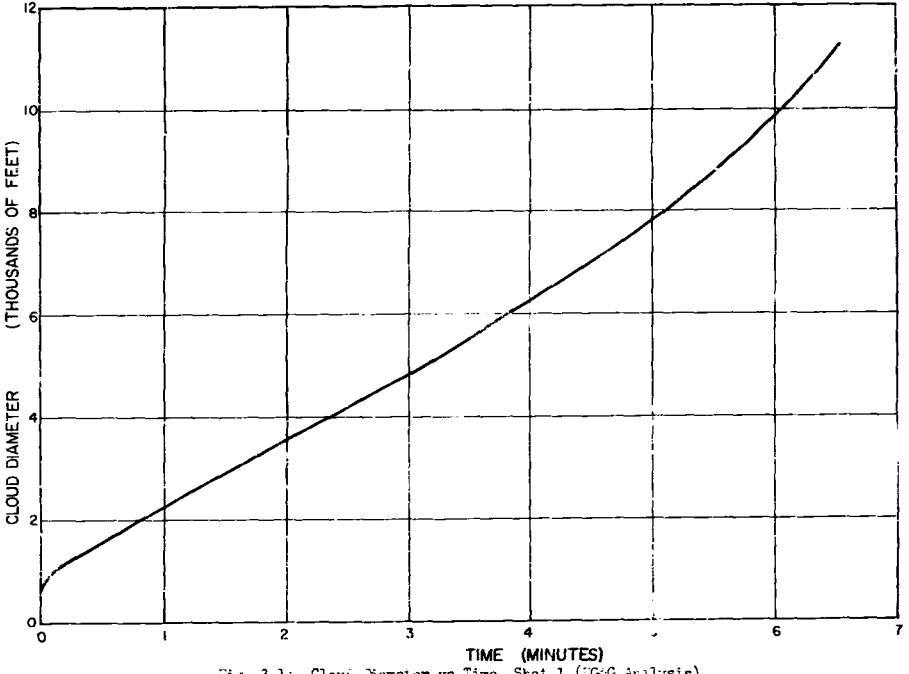

Fig. 3.1: Cloud Diameter vs Time, Shot 1 (EG&G Analysis)

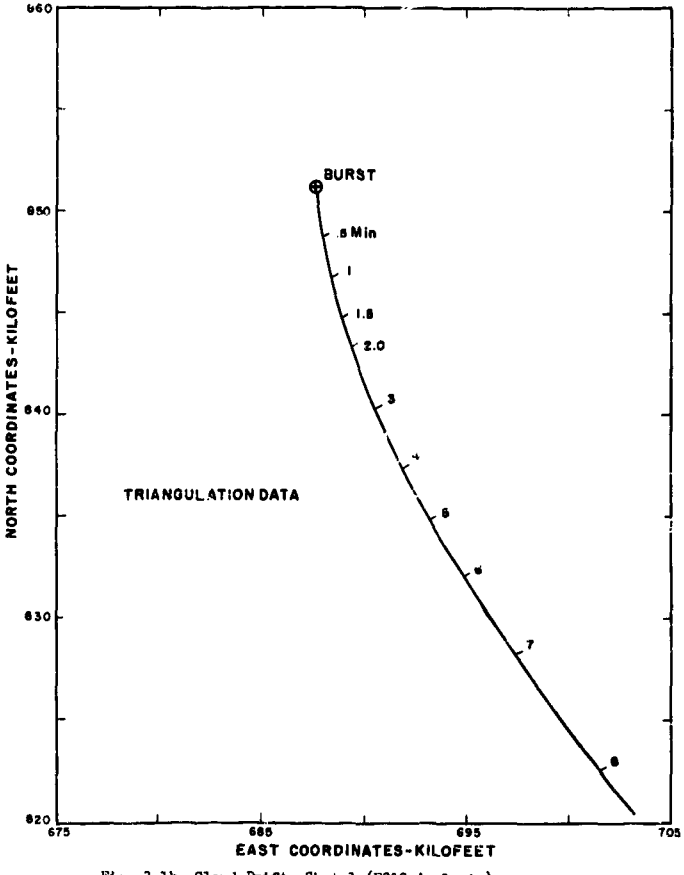

Fig. 3.1b Cloud Drift, Shot 1 (EG&G Analysis)

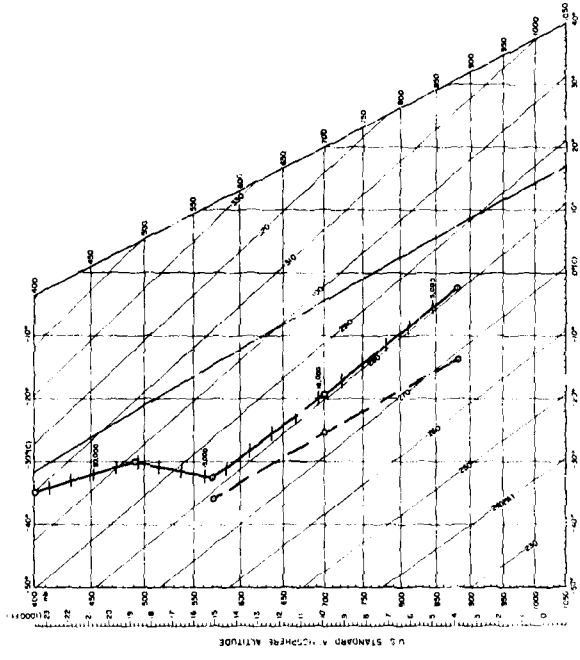

Fig. 3.2 Pseudo-Adiabatic Chart, Shot 1

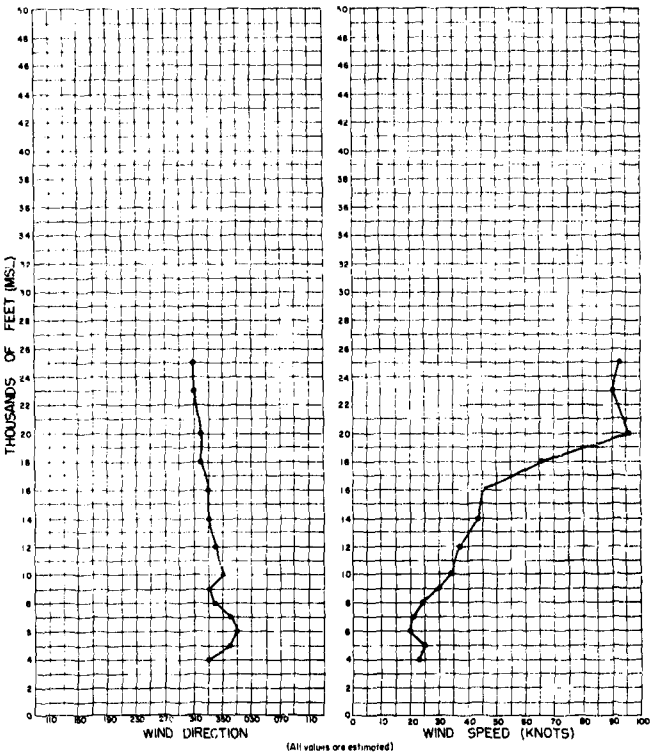

Fig. 3.3 Wind Speed and Direction, Shot 1

3.2 SHOT 2

3.2.1 Edgerton, Germeshausen & Grier Photographic Analysis

The cloud height vs time curves and diameter, Figs. 3.4* and 3.4a, were calculated as a result of measurements made on original negatives from cloud tracking stations at Amargosa and Mt. Charleston (Angel's Peak). Drift of the cloud was determined by triangulation (Fig. 3.4b).

3.2.2 Aircraft Reports (See Fig. 3.4)

With the assistance of the 4926th Sampling Squadron, the following cloud data on this shot were obtained: H + 10 min - 24,880 ft MSL top of cloud, 17,000 ft MSL base of cloud; H + 20 min - 24,000 ft top of cloud; H + 48 min - 17,000 ft base of cloud, tail lowering to 15,000 ft MSL.

3.2.3 Theodolite Data

Theodolite Location: Control Point (4,140 ft MSL)
Horizontal Distance to Burst Point: 42,402 ft
Bearing to Burst Point (from theodolite): 13.328°
Elevation of Burst: 4325 ft MSL

3.2.4 Comparison of Cloud Height Observations

Figure 3.4 indicates good agreement on reported maximum height of cloud as reported by photography, theodolite, and aircraft. The rate of rise from the theodolite reading appears too extreme with no apparent reason. One possible explanation would be the predawn shot time, making it difficult to record accurately the initial theodolite readings.

TABLE 3.2 - Theodolite Data, Shot 2

Time (min)	Elevation Angle	Horizontal Distance (ft)	Cloud Height (ft MSL)
0	-	42,402	4,325
1.3	5.2	43,600	8,200
2.5	23.7	40,500	22,000
3.0	25.6	40,000	23,500
3.8	26.8	39,250	24,100
4.5	27.6	39,100	24,700
5.0	26.9	39,250	24,100
6.0	26.2	40,250	24,100
7.0	25.5	42,100	24,500
9.5	21.2	49,800	23,600

* Fig. 3.4 curve is constructed as the best fit curve from computed points not indicated on this chart.

TABLE 3.3 - Theodolite Data, Shot 3

Time (min)	Elevation Angle	Horizontal Distance (ft)	Cloud Height (ft MSL)
0	-	69,400	4,501
1.5	10.0	69,250	16,400
2.0	12.0	69,400	18,900
3.0	14.0	69,200	21,300
4.0	15.5	69,100	23,300
5.0	17.5	68,900	25,900
6.0	19.3	69,100	28,400
7.0	20.0	69,500	29,300
8.0	20.3	69,750	30,000
9.0	20.4	70,500	30,400
10.0	20.1	71,200	30,300
11.0	19.5	72,000	29,700
12.0	19.0	72,900	29,200

TABLE 3.4 - Theodolite Data, Shot 4

Time (min)	Elevation Angle	Horizontal Distance (ft)	Cloud Height (ft MSL)
0.0		76,479	4,991
1.0	11.9	76,300	20,250
2.0	16.2	76,300	26,220
2.5	19.4	76,400	32,070
3.5	24.4	75,850	38,360
4.0	25.2	75,800	39,850
4.5	26.6	75,600	42,050
5.0	27.1	75,450	42,770
5.5	27.6	75,100	43,360
6.0	27.9	74,800	43,770
6.5	28.5	74,500	44,620
7.0	27.8	74,250	43,320
7.5	27.9	74,100	43,370
8.0	29.0	74,100	45,170
9.0	29.2	73,650	45,270
9.5	29.6	73,600	46,970
10.0	29.6	73,650	47,000

3.2.5 Weather Data

Clouds: 1/10 altocumulus 12,000 ft; 5/10 cirrostratus 30,000 ft
Visibility: 15 mi
Weather: None
Shot Height (4325 ft MSL): Temperature, -3.9°C; Pressure, 871 mb; Potential Temperature, 290°K
Pseudo-Adiabatic Chart: See Fig. 3.5
Vertical Wind Speed and Direction: See Fig. 3.6

3.2.6 Comparison of Weather Data and Cloud Evaluation

Compared to past test data, the height attained by this cloud, after adjusting yield to sea level, appears to be in excess by 2000 to 3000 ft. Examination of the lapse rate curve indicates a generally stable condition which does not suggest any reason for an excess height for the cloud. The wind speed chart indicates increase of wind with height up to 30,000 ft.

3.3 SHOT 3

3.3.1 Edgerton, Germeshausen & Grier Photographic Analysis

The curves plotted in Figs. 3.7* and 3.7a are the result of measurements made from camera stations at Amargosa and Mt. Charleston. Drift of the cloud was determined by triangulation (Fig. 3.7b).

3.3.2 Aircraft Reports (See Fig. 3.7)

The following cloud information was obtained from the 4926th Test Sampling Squadron, AFSWC: H + 8 min - 30,000 ft top (MSL); H + 13 min - 18,000 ft base (MSL); H + 49 min - 27,000 ft top (MSL).

3.3.3 Theodolite Data

Theodolite Location: Control Point (4127 ft MSL)
Horizontal Distance to Burst Point: 69,400 ft
Bearing to Burst Point: 1.6°C
Burst Height: 4501 ft MSL

3.3.4 Comparison of Cloud Height Observations

The aircraft, theodolite, and photographic data appear to agree quite well. The deviation of the theodolite data from the EG&G rate of rise (Fig. 3.7) is expected considering the accuracy of theodolite measurements.

3.3.5 Weather Data

Clouds: None
Visibility: 15 mi
Weather: None
Shot Height (4501 ft MSL): Temperature, -0.5°C; Pressure, 864 mb; Potential Temperature, 284°K
Pseudo-Adiabatic Chart: See Fig. 3.8
Wind Speed and Direction: See Fig. 3.9

3.3.6 Comparison of Weather Data and Cloud Height

The maximum height reached by the cloud agrees well with a curve of past cloud data (using adjusted yield). The lapse rate curve

* Fig. 3.7 curve is constructed as the best fit curve from computed points not indicated on this chart.

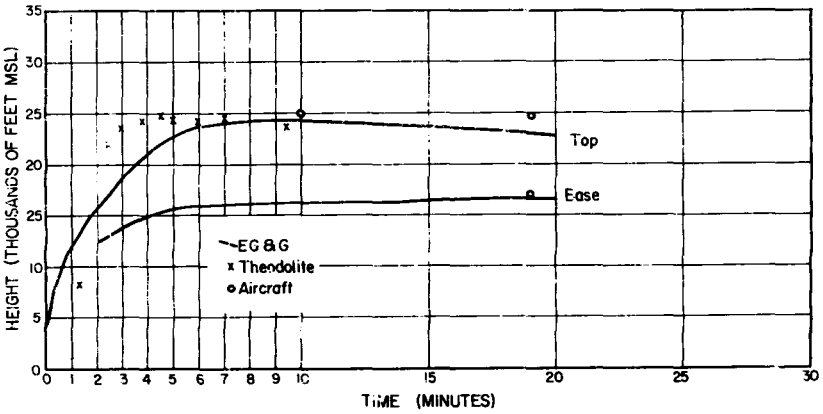

Fig. 3.4 Cloud Rise vs Time, Shot 2

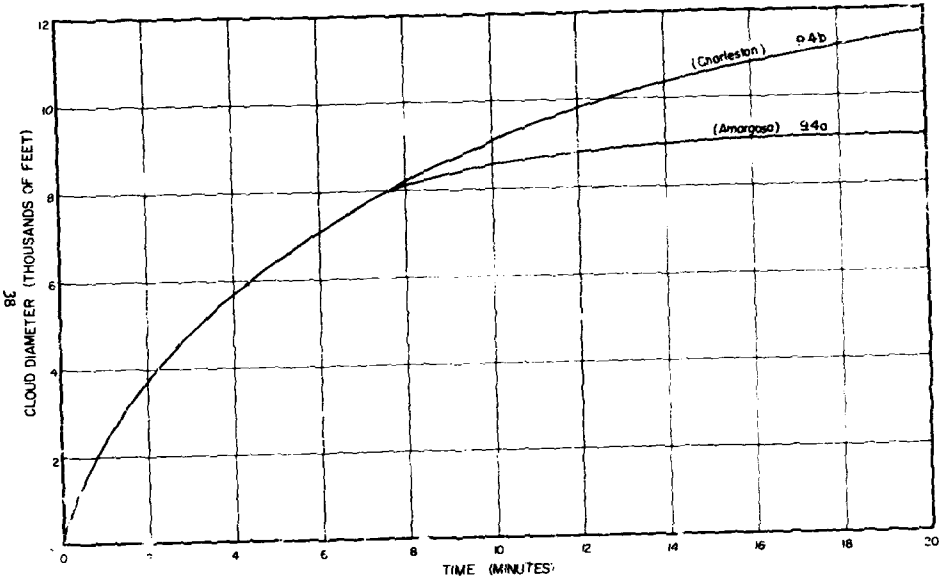

Fig. 3.4a Cloud Diameter vs Time, Shot 2 (EG&G Analysis)

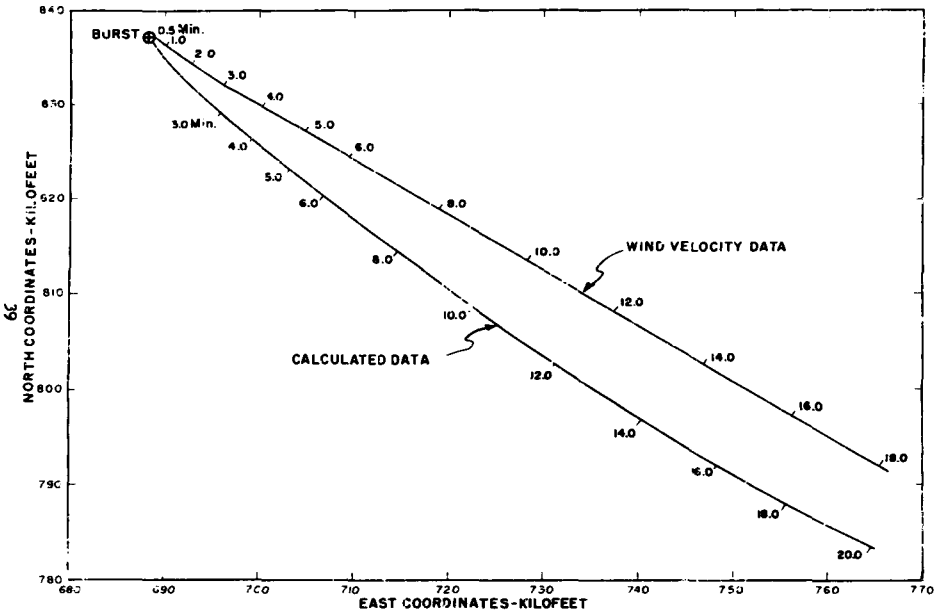

Fig. 3.4b Cloud Drift, Shot 2 (EG&G Analysis)

indicates an isothermal layer between 4900 to 8000 ft MSL which did not appear to influence the cloud rise. The wind speed was westerly and generally constant below 17,000 ft and above 20,000 ft.

3.4 SHOT 4

3.4.1 Edgerton Germeshausen & Grier Photographic Analysis

Camera locations at Amargosa and Angel's Peak recorded data used in computing Figs. 3.10,* 3.10a, and 3.10b.

3.4.2 Aircraft Reports (See Fig. 3.10)

Sampling aircraft reported the following cloud data: H + 30 min - 40,500 ft MSL top; H + 100 min - 41,000 ft MSL top.

3.4.3 Theodolite Data

Theodolite Location: Control Point (4,127 ft MSL)
Horizontal Distance to Burst Point: 76,479 ft
Bearing to Burst Point: 346.089°
Burst Height: 4991 ft MSL

3.4.4 Comparison of Cloud Height Observations

The theodolite data suggest higher cloud heights than the more valid photographic analysis. This discrepancy is due to the error in reading the apparent cloud top but, in effect, reading a point which actually is the side of cloud. This error is due to the increase in mushroom size and wind shift.

3.4.5 Weather Data

Clouds: Clear
Visibility: Unrestricted
Weather: None
Shot Height (4991 ft): Temperature, 5.6°C; Pressure, 856 mb; Potential Temperature, 291°K
Pseudo-Adiabatic Chart: See Fig. 3.11
Wind Speed and Direction: See Fig. 3.12

3.4.6 Comparison of Cloud Data and Weather Data

The past cloud height data (see Fig. 1.1) is in good agreement with the height reached by this cloud. The lapse rate curve is quite stable to 9000 ft but obviously did not influence the rise of the cloud. The remainder of the curve to 40,000 ft also appears stable. The height of the tropopause at 40,000 ft would suggest a barrier to further significant rise.

* Fig. 3.10 curve is constructed as the best fit curve from computed points not indicated on this chart.

Fig. 3.5 Pseudo-Adiabatic Chart, Shot 2

TABLE 3.5 - Theodolite Data, Shot 5

Time (min)	Elevation Angle	Horizontal Distance (ft)	Cloud Height (ft MSL)
0.0	-	39,440	4,313
0.5	6.9	39,440	8,910
1.0	12.2	39,440	12,530
1.5	16.4	39,400	15,750
2.0	19.6	39,400	18,360
2.5	22.4	39,200	20,320
3.0	24.7	39,150	22,190
3.5	26.8	39,350	24,040
4.0	29.4	39,600	26,440
4.5	30.7	39,740	27,440
5.5	32.6	39,970	29,440
6.0	33.6	40,230	30,840
7.0	34.7	41,000	32,330
9.5	34.4	45,350	35,180
12.0	32.2	51,720	36,690
13.5	30.6	55,350	37,410
14.5	29.3	57,450	37,540
15.5	28.2	59,100	37,990
17.0	26.5	61,700	38,390
18.0	24.6	73,800	38,470
19.5	24.1	78,750	39,300

TABLE 3.6 - Theodolite Data, Shot 6

Time (min)	Elevation Angle	Horizontal Distance (ft)	Cloud Height (ft MSL)
0.0	-	59,024	4,745
1.0	19.5	59,200	14,800
2.0	16.7	56,600	21,800
3.0	23.9	54,200	28,800
4.0	28.3	52,400	32,900
5.0	32.5	51,500	37,600
6.0	35.3	50,300	40,400
7.0	38.0	50,400	44,200
8.0	39.8	52,000	48,100
9.0	40.1	54,000	50,300
10.5	39.3	58,000	52,800
13.0	38.9	64,600	56,900
15.0	34.6	71,800	54,300

3.5 SHOT 5

3.5.1 Edgerton, Germeshausen & Grier Photographic Analysis

The data indicated in Figs. 3.14* and 3.14a were computed from camera records collected at Amargosa and Mt. Charleston (Angel's Peak) stations. Calculations were based upon photogrammetric triangulation, including cloud drift in Fig. 3.14b.

3.5.2 Aircraft Reports

Sampling aircraft reported the following cloud data: H + 37 min - 36,000 ft top; 27,000 to 28,000 ft base (estimate).

3.5.3 Theodolite Data

Theodolite Location: Control Point
Horizontal Range to Burst Point: 39,440 ft
Bearing to Burst Point: 12.443°
Height of Burst: 4313 ft MSL

3.5.4 Comparison of Cloud Height Observations

Theodolite and photo measurements appear to have good agreement. The later theodolite readings (after 12 min) probably give higher values because the side, rather than top, of the cloud was being measured.

3.5.5 Weather Data

Clouds: Clear
Visibility: Unrestricted
Weather: None
Shot Height (4313 ft): Temperature, 2.0°C; Pressure, 874 mb; Potential Temperature, 286°K
Pseudo-Adiabatic Chart: See Fig. 3.15
Wind Speed and Direction: See Fig. 3.16

3.5.6 Comparison of Cloud and Weather Data

The height attained by this cloud was in excess of 10,000 ft greater than expected. The lapse rate curve is generally stable throughout the layer. The wind direction is fairly consistent from 270°. The speed is relatively light (below 20 knots) to 18,000 ft and not above 30 knots to 26,000 ft.

* Fig. 3.14 curve is constructed as the best fit curve from computed points not indicated on this chart.

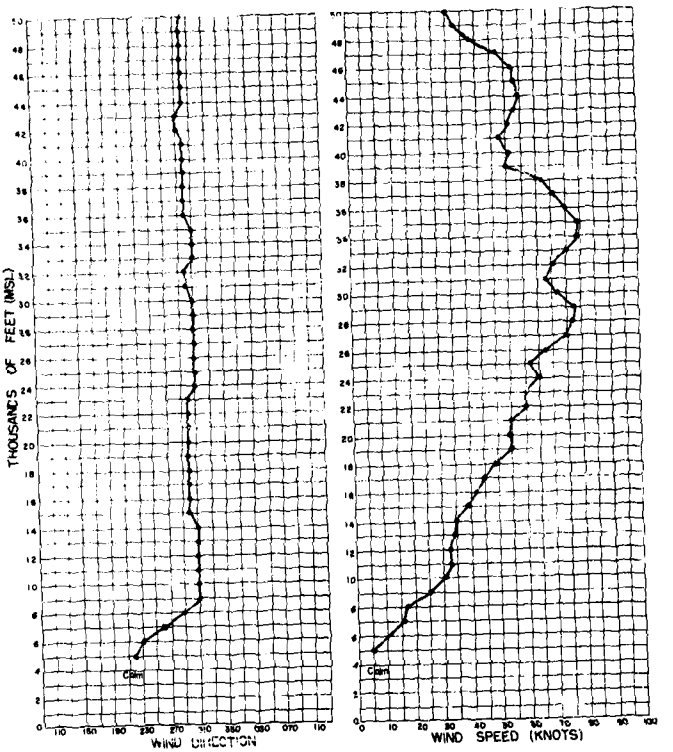

Fig. 3.6 Wind Speed and Direction, Shot 2

3.6 SHOT 6

3.6.1 Edgerton, Germeshausen & Grier Photographic Analysis

Cloud data were computed from camera stations located at Amargosa and Mt. Charleston (Angel's Peak). Figures 3.17* and 3.17a are the result of such analysis, as well as Fig. 3.17b.

3.6.2 Aircraft Reports (See Fig. 3.17)

Sampling aircraft reported the following cloud data: H 13 min - 40,000 ft top of cloud; H 18 min - 38,400 ft top of cloud, 34,300 ft base of cloud; H + 22 min - 32,200 ft base of cloud; H + 47 min - 39,200 ft top of cloud, 36,900 ft base of cloud.

3.6.3 Theodolite Data

Theodolite Location: Control Point
Horizontal Distance to Burst Point: 59,024 ft
Bearing to Burst Point: 8.735°
Burst Height: 4745 ft MSL

3.6.4 Comparison of Cloud Height Observations

This shot is the best example of this series of the problems inherent in theodolite measurements when the cloud drift is clearly toward the observation point. The theodolite readings are obviously affected by this condition and are of no value after 4 min. To compensate for this effect, a correction for cloud diameter must be made. Aircraft reports on cloud top agree with photographic measurements. The discrepancy in base estimate is due to the multiple layers of the cloud causing a question as to just what constitutes the base.

3.6.5 Weather Data

Clouds: None
Visibility: Unrestricted
Weather: None
Shot Height (4745 ft): Temperature, 4.5°C; Pressure, 860 mb; Potential Temperature, 288°K
Pseudo-Adiabatic Chart: See Fig. 3.18
Wind Speed and Direction: See Fig. 3.19

3.6.6 Comparison of Cloud and Weather Data

The cloud rise was about 7000 ft higher than indicated by past data (adjusted yield). The lapse rate does not suggest any marked instability; in fact, is stable from 13,000 ft to the cloud top. The tropopause at 36,500 ft should have dampened any further rise of more than a few thousand feet. The wind speed from 20,000 ft to cloud top

* Fig. 3.17 curve is constructed as the best fit curve from computed points not indicated on this chart.

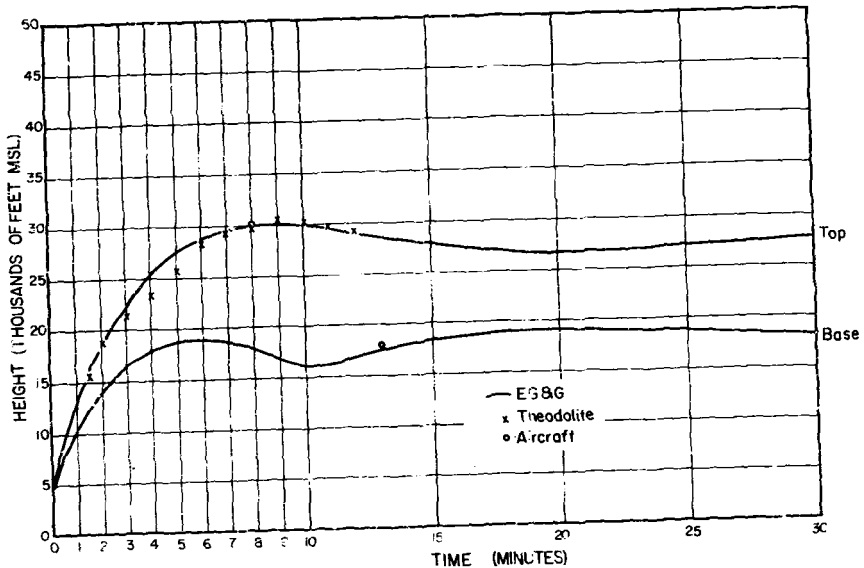

Fig. 3.7 Cloud Rise vs Time, Shot 3

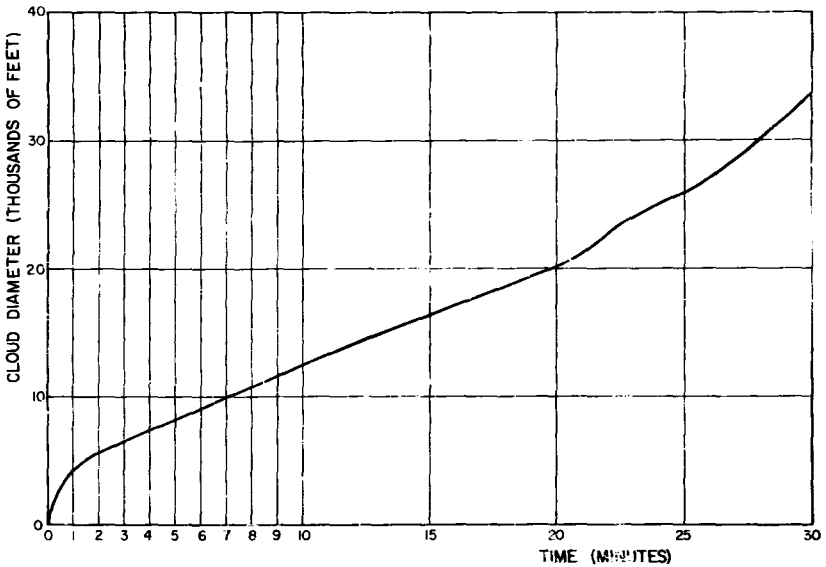

Fig. 3.7a Cloud Diameter vs Time, Shot 3 (EG&G Analysis)

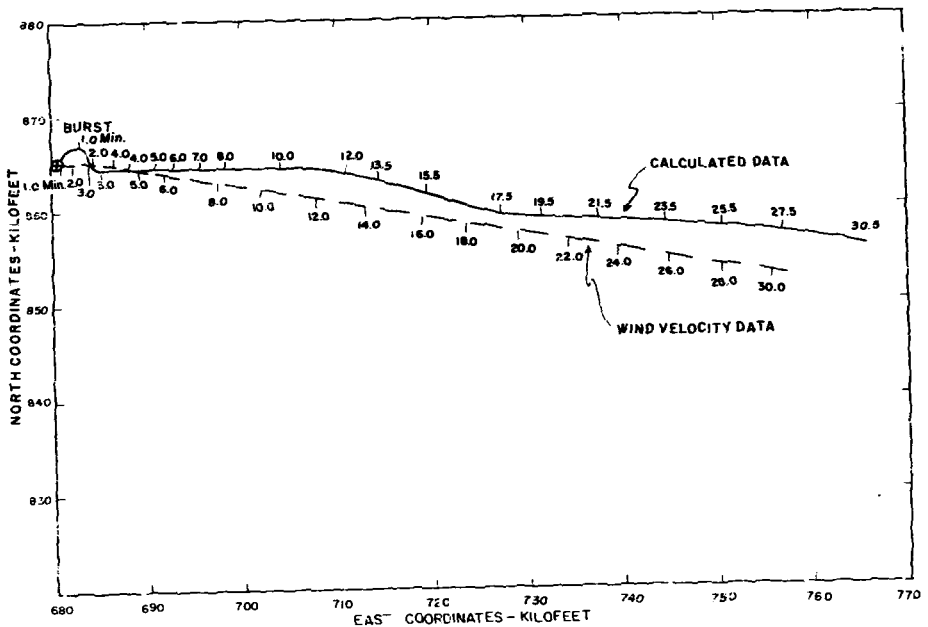

Fig. 3.7b Cloud Drift, Shot 3 (EG&G Analysis)

TABLE 3.7 - Theodolite Data, Shot 7

Time (min)	Elevation Angle	Horizontal Distance (ft)	Cloud Height (ft MSL)
0.0	-	85,176	-
0.5	1.6	85,176	6,687
1.0	2.3	84,650	7,540
1.5	2.8	84,125	8,350
2.0	3.2	84,000	8,830
2.5	3.6	83,100	9,290
3.0	3.9	82,500	9,770
3.5	4.3	82,100	10,240
4.0	4.6	81,400	10,770
4.5	4.9	80,400	11,090
5.0	5.2	79,600	11,420
5.5	5.4	78,900	11,560
6.0	5.4	78,000	11,510
6.5	5.4	77,000	11,440
7.0	5.3	76,000	11,140
7.5	5.2	75,200	11,030
8.0	5.1	74,400	10,780
8.5	5.0	74,000	10,540
9.5	4.8	72,900	10,140
11.5	4.0	71,900	9,170

TABLE 3.8 - Theodolite Data, Shot 8

Time (min)	Elevation Angle	Horizontal Distance (ft)	Cloud Height (ft MSL)
0.0	-	60,265	4,809
1.0	10.0	61,300	14,940
2.0	15.3	61,250	20,690
3.0	18.7	60,250	24,520
4.0	20.9	59,250	26,750
5.0	22.0	59,200	27,920
6.0	23.1	59,400	29,440
7.0	23.3	60,100	30,020
8.0	23.1	61,000	30,140
9.0	22.8	62,300	30,350
10.0	22.3	63,900	30,350
11.0	21.3	65,800	29,750
12.0	20.8	67,900	29,900
13.0	20.2	70,250	29,950
14.0	19.3	72,600	29,550
15.0	18.1	75,250	29,750

is fairly consistent (about 40 knots) and does not indicate any noticeable shear.

3.7 SHOT 7

3.7.1 Edgerton, Germeshausen & Grier Photographic Analysis

No data were compiled for this underground shot.

3.7.2 Aircraft Reports (See Fig. 3.20)

Sampling aircraft reported the following cloud data: H + 10 min - 12,000 ft MSL; H + 12 min - 10,500 ft MSL.

3.7.3 Theodolite Data

Theodolite Location: Control Point
Horizontal Distance to Burst Point: 85,176 ft
Bearing to Burst Point: 2.094°
Burst Height: 67 ft below surface (4221 ft MSL)

3.7.4 Comparison of Cloud Height Observations

No EG&G data are available for this shot. Reasonable agreement is indicated between aircraft and theodolite measurements considering the questionable accuracy of the latter after the first few minutes.

3.7.5 Weather Data

Clouds: 3/10 thin cirrus
Visibility: Unrestricted
Weather: None
Shot Height (Surface Data): Temperature, 17.0°C; Pressure 883 mb; Potential Temperature, 301°K
Pseudo-Adiabatic Chart: See Fig. 3.21
Wind Speed and Direction: See Fig. 3.22

3.7.6 Comparison of Weather and Cloud Data

Although a subsurface burst does not lend itself too well to comparison to other shots relative to maximum height attained, an examination can be made relative to its evolution. The lapse rate curve indicated a small inversion from about 9000 to 10,000 ft which roughly coincided with the maximum height reached; also, an unstable layer from surface to 8000 ft. The wind speed increased 10 mi an hr and direction changed 17° from 10,000 to 12,000 ft suggesting the effect of a shear.

3.8 SHOT 8

3.8.1 Edgerton, Germeshausen & Grier Photographic Analysis

Figures 3.23* and 3.23a were derived from data recorded at the Amargosa and Mt. Charleston camera locations; also Fig. 3.23b.

* Fig. 3.23 curve is constructed as the best fit curve from computed points not indicated on this chart.

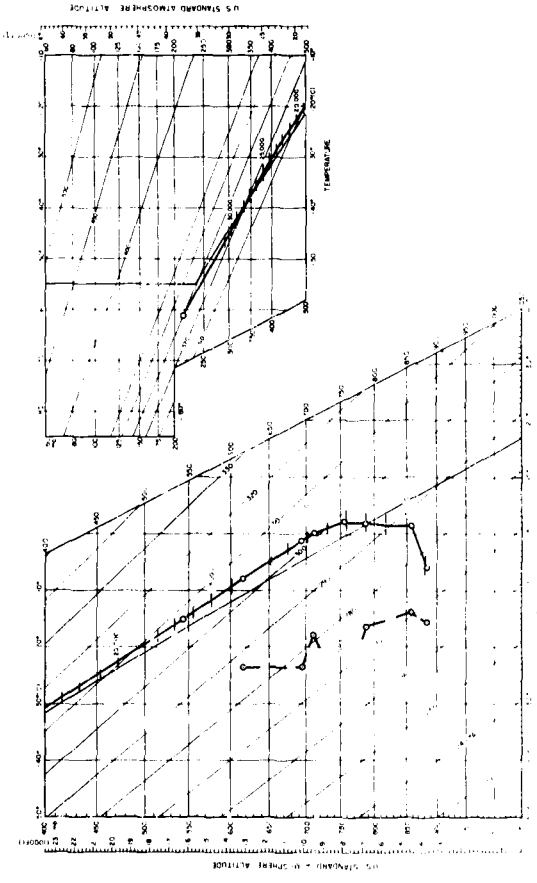

Fig. 3.6 Pseud.-Adiabatic Chart, Shot 3

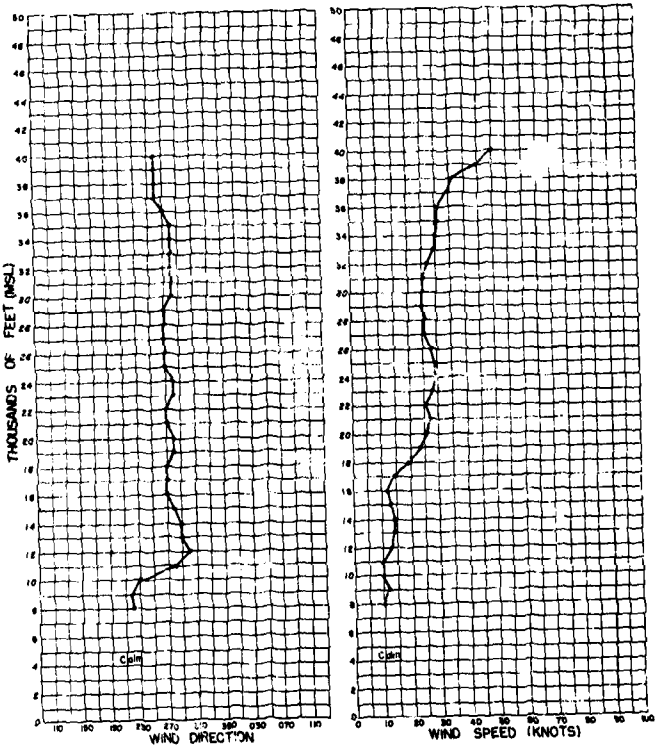

Fig. 3.9 Wind Speed and Direction, Shot 3

3.8.2 Aircraft Reports (See Fig. 3.23)

Sampling aircraft reported the following cloud data: H+10 min - 31,200 ft top; H+15 min - 30,700 ft top; H+17 min - 22,800 ft base; H+30 min - 29,000 ft top; H+44 min - 18,000 ft base.

3.8.3 Theodolite Data

Theodolite Location: Control Point
Horizontal Distance to Burst Point: 60,265 ft
Bearing to Burst Point: 346.389°
Burst Height: 4809 ft MSL

3.8.4 Comparison of Cloud Height Observations

Photographic, aircraft, and theodolite data agree quite well. The sense of the discrepancy between the theodolite and other measurements is contrary to what is usually found. This may be due to the fact that the wind shears diluted the cloud top, making it too faint to identify.

3.8.5 Weather Data

Clouds: None
Visibility: Unrestricted
Weather: None
Shot Height (4809 ft MSL): Temperature, 9.3°C; Pressure, 852 mb; Potential Temperature, 295°K
Pseudo-Adiabatic Chart: See Fig. 3.24
Wind Speed and Direction: See Fig. 3.25

3.8.6 Comparison of Weather Data and Cloud Data

The lapse rate curve indicates a stable layer from 8200 to 11,000 ft with an inversion from 11,000 to 11,600 ft. The rest of the curve is generally unstable to height of cloud top. The wind speed is irregular with increases and decreases from 10,000 to 25,000 ft.

3.9 SHOT 9

3.9.1 Edgerton, Germeshausen & Grier Photographic Analysis

Quality of photographic data was unsuitable for analysis.

3.9.2 Aircraft Reports (See Fig. 3.27)

Sampling aircraft reported the following cloud data: H+10 min - 27,500 ft (MSL) top of cloud: H+17 min - 31,500 ft (MSL) top of cloud: H+24 min - 28,700 ft (MSL) top of cloud.

3.9.3 Theodolite Data

Theodolite Location: Control Point
Horizontal Distance to Burst Point: 56,147 ft
Bearing to Burst Point: 9.758°
Burst Height: 4995 ft MSL

3.9.4 Comparison of Cloud Height Observations

Comparison of data for this shot is impossible since no photographic data are available and the theodolite and aircraft data are not simultaneous.

3.9.5 Weather Data

Clouds: 7/10 thin cirrostratus
Visibility: Unrestricted
Weather: None
Shot Height (4995 ft MSL): Temperature, 12.4°C; Pressure, 845 mb; Potential Temperature, 300°K
Pseudo-Adiabatic Chart: See Fig. 3.28
Wind Speed and Direction: See Fig. 3.29

3.9.6 Comparison of Cloud Data and Weather Data

No photographic analysis was made on this shot. On the basis of theodolite and aircraft reports alone, the cloud appears to have risen about 5000 ft in excess of expected rise by means of past test data. The lapse rate curve is generally unstable to 8500 ft. However, an inversion from 8500 to 9600 ft would tend to decrease the height. The wind direction is generally consistent and the speed increases above 10,000 ft to 30,000 ft.

3.10 SHOT 10

3.10.1 Edgerton, Germeshausen & Grier Photographic Analysis

Figures 3.30,* 3.30a, and 3.30b were derived from data recorded at the Amargosa camera location only. Data from other camera locations were not obtained or were not valid due to proximity to cloud formation.

3.10.2 Aircraft Reports (See Fig. 3.30)

Sampling aircraft reported the following cloud data: H + 0 min - 60,000 to 65,000 ft top (estimate); H + 45 min - 65,000 ft top (estimate).

3.10.3 Theodolite Data

Theodolite Location: 25 ft north of main road entering Frenchman Flat area, about 200 ft east of the Mercury Highway (3220 ft MSL)
Horizontal Distance to Burst Point: 82,272 ft
Bearing to Burst Point: 349°62.5'
Burst Height: 36,620 ± 60 ft MSL

* Fig. 3.30 curve is constructed as the best fit curve from computed points not indicated on this chart.

TABLE 3.9 - Theodolite Data, Shot 9

Time (min)	Elevation Angle	Horizontal Distance (ft)	Cloud Height (ft MSL)
0.0	-	56,150	4,995
0.5	5.3	56,150	9,360
1.0	8.8	57,250	13,010
1.5	9.9	58,400	14,360
2.0	11.4	59,700	16,320
2.5	12.8	60,800	17,940
3.0	13.1	61,850	18,740
3.5	15.0	63,150	21,080
4.0	15.6	64,450	22,110
4.5	16.2	65,450	23,170
5.0	16.7	66,700	24,140
5.5	17.1	68,350	25,160
6.0	17.4	70,200	26,120
6.5	17.6	72,150	27,020
7.0	17.8	74,200	27,950
7.5	17.8	76,300	28,640
8.0	17.8	78,650	29,370
9.0	17.7	83,250	30,610
10.0	17.3	88,500	31,740

TABLE 3.10 - Theodolite Data, Shot 10*

Time (min)	Elevation Angle	Horizontal Distance (ft)	Cloud Height (ft MSL)
0	-	82,250	36,600
1.0	27.0	78,400	42,800
2.0	30.5	74,500	47,100
3.0	30.5	72,250	50,100
4.0	34.3	71,700	52,100
5.0	(34.6)	(72,500)	(53,200)
6.0	(34.6)	(74,000)	(54,200)
7.0	(34.3)	(75,700)	(54,800)

*Parentheses indicate data of doubtful accuracy.

The cloud had a torus ring appearance and began to disintegrate at 4 min. The short life of the visible cloud was due to lack of moisture at the burst level. Because readings were taken on the edge of the ring, an estimate then had to be made of the elevation of the center of the ring for true height of the cloud.

3.10.4 Comparison of Cloud Height Observations

Despite the doubtful accuracy of the theodolite readings the computed heights compare favorably with the photographically-determined heights. The aircraft estimates do not agree but can be considered doubtful due to the ceiling limitations of the sampling aircraft.

3.10.5 Weather Data

Clouds: Clear
Visibility: Unrestricted
Weather: None
Burst Height (36,620 ft MSL): Temperature, -47.7°C; Pressure 222 mb; Potential Temperature, 347°K
Pseudo-Adiabatic Chart: See Fig. 3.31
Wind Speed and Direction: See Fig. 3.32

3.10.6 Comparison of Cloud Data and Weather Data

The predicted height for this cloud was underestimated by some 10,000 ft. The lapse rate curve indicates that the burst was in the stratosphere. The lack of moisture in the ambient stratosphere should tend to reduce the size of the apparent cloud and hence its maximum height. The former was observed but the latter did not materialize. Also, the isothermal layer between 33,000 and 40,000 ft should have served a further deterrent to its rise. It becomes apparent that the height prediction equations omit some pertinent atmospheric parameter or parameters affecting the amount of rise of atomic clouds, particularly in a stratospheric environment. The wind direction was generally uniform from burst point through the maximum height of 55,000 ft.

3.10.7 Army Map Service Volume Analysis

The photography of the high altitude shot was evaluated upon receipt at AMS. The photography was satisfactory from the standpoint of photographic quality but the air burst did not provide enough "substance" to enable a good photographic image to be registered. The lack of density in the residual cloud precludes photogrammetric determinations of volume in this type of shot.

3.11 SHOT 11

3.11.1 Edgerton, Germeshausen & Grier Photographic Analysis

The data indicated in Figs. 3.34* and 3.34a were computed from camera records collected at Amargosa and Angel's Peak. Photogrammetric triangulation was used for calculations, as well as for Fig. 3.34b.

* Fig. 3.34 curve is constructed as the best fit curve from computed points not indicated on this chart.

3.11.2 Aircraft Reports (See Fig. 3.34)

Sampling aircraft reported the following cloud data: H + 12 min - 15,200 ft MSL top; H + 15 min - 15,000 ft MSL top; H + 22 min - 13,000 ft MSL base; H + 30 min - 15,000 ft MSL top; H + 30 min - 13,000 ft MSL base.

3.11.3 Theodolite Data

Theodolite Location: Control Point
Horizontal Distance to Burst Point: 68,534 ft
Bearing to Burst Point: 4.9°
Burst Height: 4542 ft MSL

3.11.4 Comparison of Cloud Height Observations

Aircraft, camera, and theodolite measurements give good agreement.

3.11.5 Weather Data

Clouds: Clear
Visibility: Unrestricted
Weather: None
Burst Height (4542 ft MSL): Temperature, 4.5°C; Pressure, 867 mb; Potential Temperature, 285°K
Pseudo-Adiabatic Chart: See Fig. 3.35
Wind Speed and Direction: See Fig. 3.36

3.11.6 Comparison of Cloud Data and Weather Data

The cloud rose slightly higher than expected. The lapse rate curve indicates an inversion to 5000 ft, and then lies between the dry and moist adiabatic curve throughout. The wind direction was from the NNW-N with a wind speed increase up to 35,000 ft.

3.11.7 Army Map Service Volume Analysis

The photography of Shot 11 was evaluated upon receipt at AMS and was found to be a complete loss. No useful photographic images were obtained due to the lack of light at the time of the shot.

3.12 SHOT 12

3.12.1 Edgerton, Germeshausen & Grier Photographic Analysis

Figures 3.37* and 3.37a were derived from camera records collected at Amargosa and Angel's Peak. Figure 3.37b was computed from the same records.

* Fig. 3.37 curve is constructed as the best fit curve from computed points not indicated on this chart.

3.12.2 Aircraft Reports (See Fig 3.37)

Sampling aircraft reported the following cloud data: H + 11 min - 41,500 to 41,700 ft top of cloud; H + 23 min - 41,700 ft top of cloud; H + 32 min - 42,800 ft top of cloud.

3.12.3 Theodolite Data

Theodolite Location: Control Point
Horizontal Distance to Burst Point: 61,859 ft
Bearing to Burst Point: 143.525°
Burst Height: 3477 ft MSL

3.12.4 Comparison of Cloud Height Observations

Camera, theodolite and aircraft data agree quite well on maximum height.

3.12.5 Weather Data

Clouds: Clear
Visibility: 15 mi
Weather: None
Shot Height (3477 ft MSL): Temperature, 18.5°C; Pressure, 880 mb; Potential Temperature, 302°K
Pseudo-Adiabatic Chart: See Fig. 3.38
Wind Direction and Speed: See Fig. 3.39

3.12.6 Comparison of Cloud and Weather Data

The lapse rate curve indicates small inversions at approximately 10,000 ft and 21,000 ft which did not appear to affect the cloud rise. Unstable layers occur from surface to 10,000 ft and 16,000 to 21,000 ft. The maximum cloud height seems to have occurred at the tropopause height. The wind speed data indicate a strong shear between 20,000 to 25,000 ft.

3.12.7 Army Map Service Volume Analysis

The photographic materials of Shot 12 were inspected upon receipt and were found to be of good quality. The image of the cloud was good on all exposures except the initial photograph which was completely over-exposed by the intense light. These materials were found satisfactory for continuation of the planned procedures.

The orientation data listed below were determined to be the minimum necessary for use of the photography as planned. Field values are shown where available. The remainder of the necessary data was determined in the office photogrammetrically. These values are underlined.

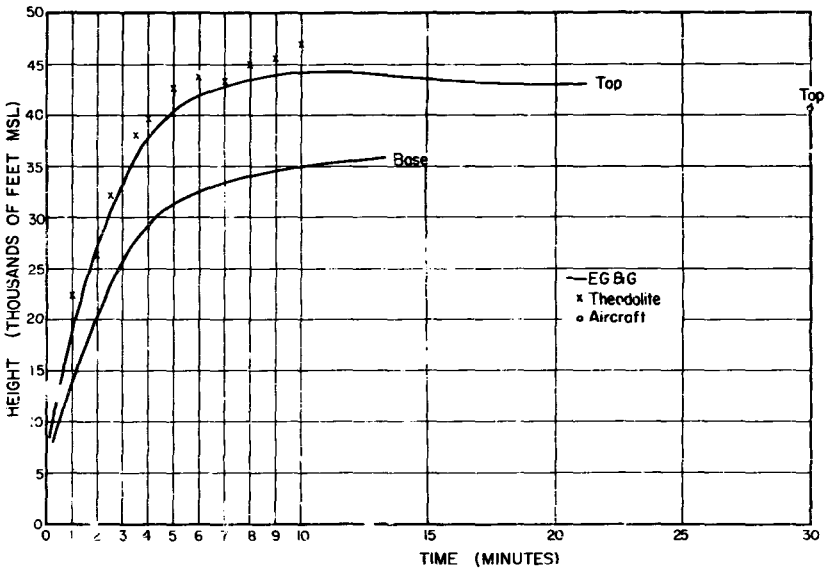

Fig. 3.10 Cloud Rise vs Time, Shot 4 (EG&G Analysis)

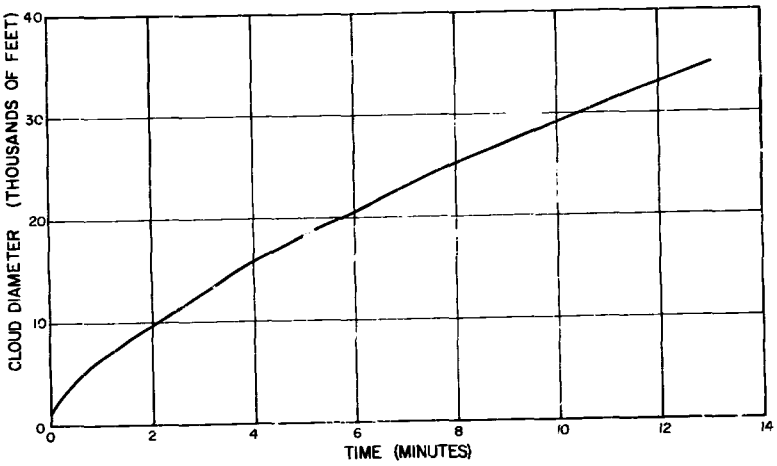

Fig. 3.10a Cloud Diameter vs Time, Shot 4 (EG&G Analysis)

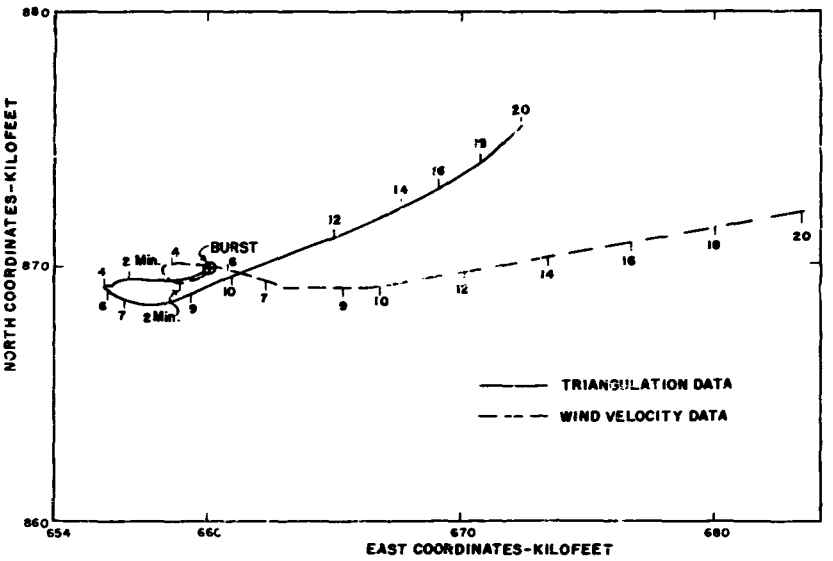

Fig. 3.10b Cloud Drift, Shot 4, (EG&G Analysis)

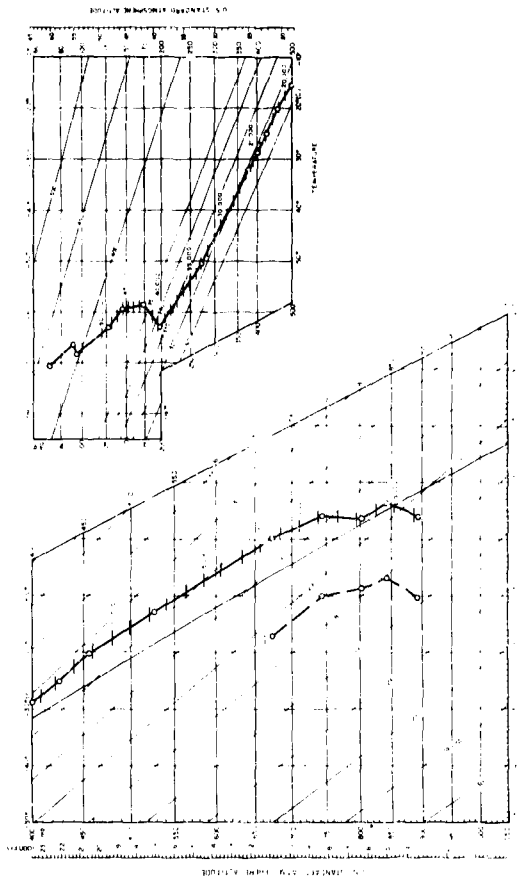

Fig. 3.11 Pseudo-Adiabatic Chart, Shot 4

TABLE 3.11 - Theodolite Data, Shot 11

Time (min)	Elevation Angle	Horizontal Distance (ft)	Cloud Height (ft MSL)
0.0	--	68,534	4,542
0.5	3.0	68,534	7,730
1.0	4.7	68,534	9,770
1.5	5.6	68,534	10,950
2.0	6.8	68,534	12,315
2.5	7.7	68,534	13,400
3.0	8.2	68,557	14,020
3.5	8.5	68,100	14,280
4.0	8.7	67,700	14,560
4.5	8.9	67,250	15,340
5.0	9.2	66,875	14,960
5.5	9.5	66,500	15,270
6.0	9.65	66,125	15,390
6.5	9.8	65,800	15,510
7.5	9.75	65,000	15,310
8.0	10.1	64,700	15,660
9.0	9.3	63,800	14,580

TABLE 3.12 - Theodolite Data, Shot 12

Time (min)	Elevation Angle	Horizontal Distance (ft)	Cloud Height (ft MSL)
0.0	-	61,859	3,477
0.5	5.8	61,859	10,420
1.0	10.6	62,200	15,790
1.5	14.3	62,550	20,040
2.0	17.2	63,000	23,660
2.5	19.6	63,875	26,720
3.0	21.9	65,000	30,220
4.0	22.6	67,800	32,340
5.0	25.1	70,950	37,340
6.0	25.7	74,250	39,720
7.0	25.3	78,100	40,990
8.0	24.3	82,250	41,240
9.0	23.0	87,100	41,020
10.0	22.1	92,000	41,490
11.0	21.1	97,200	41,540

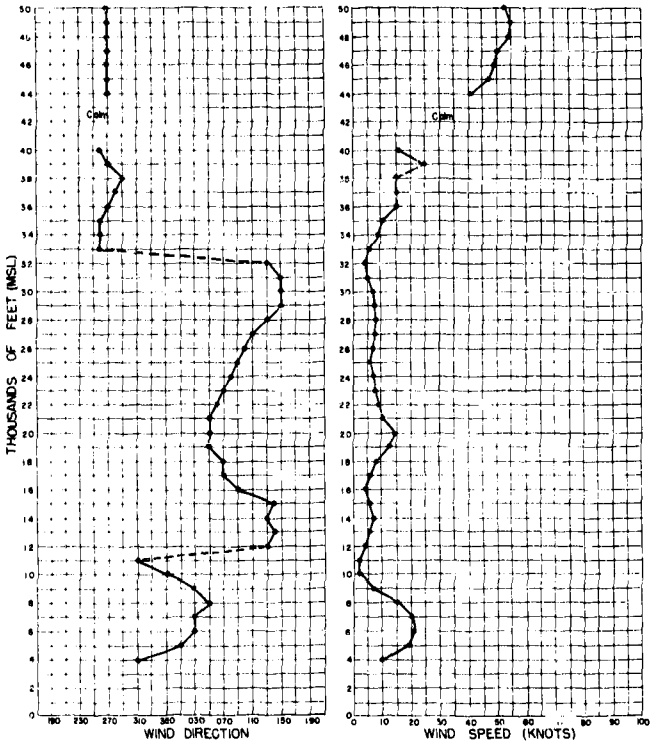

Fig. 3.12 Wind Speed and Direction, Shot 4

Geodetic Position	Camera Shot 12 West	Camera Shot 12 East	Tower
Latitude	36°43'05.3"	36°42'48.5"	36°47'53.7"
Longitude	115°58'14.7"	115°54'47.2"	115°55'44.5"
Elevation	3640 ft	3960 ft	3478 ft (top)
Inclination of camera axis from horizontal	22°36'	21°27'	
Included angle, camera axis with camera base line	72°30'	75°15'	

A pair of preshot photographs was set in the Stereoplanigraph and oriented with the aid of the above data. The orientation of a shallow depth zone centered at the tower (visible on the photographs) was satisfactory.

Phase I - A stereo pair of photographs taken at approximately zero hour + 30 sec was selected as the first test model to be set. Due to the non-synchronization of the cameras, the photographs were not taken at the same instant. The time difference could not be determined and may be as much as 3 to 5 sec.

The instrument orientation obtained with the preshot photographs was retained when the selected photographic pair was set in the instrument. This was planned to provide an oriented three dimensional model without further adjustments being required. This did not prove to be the case. However, investigation revealed that small portions of the model could be viewed, stereoscopically, by adjustment of the lateral instrument motions. This inability to form a complete three dimensional model was due to the uneven expansion of the various sections of the cloud and the time difference between the two photos used.

Phase II - The photographs used above were taken when the rate of expansion was quite rapid (about 210 ft/sec). It was felt that photographs taken later might yield better results due to a lower expansion rate. A pair of photographs taken at about zero + 2 min was placed in the instrument. In this case the expansion did appear less but the drift of the upper part of the cloud was much faster. Again only small portions (1-2 per cent of total cloud area) of the model could be oriented successfully at one time. An attempt was made to contour a portion of the cloud. It was necessary, in order to fuse the images, to constantly adjust the instrument. In this manner it was possible to keep the measuring mark on the surface of the cloud and to trace out contours of a small area. However, since the orientation of the model was not absolute, the movement of the instrument motions influenced the contour datum and each contour is not in a true plane. Even if this effect were not present the contours would not be valid contours of the cloud shape at any one instant because of the time difference between the two exposures used. It was therefore decided that further attempts to utilize this photography for stereo compilation were not feasible.

Fig. 3.13a Shot 4 Cloud (Approx H + 18 Min). Note wind shear effect.

Fig. 3.13b Shot 6 Cloud (Approx H + 6 Min). Note wind shear effect.

Phase III - During the study of the photography, the possibility arose of measuring the rate of expansion and drift of the cloud by using a series of the existing photographs from one station and superimposing the images. The drift direction of the cloud on this test has been determined, by meteorological data, to be almost perpendicular to the axis of the camera at Station Shot 12 East. This insures that the scale of the photography at the cloud distance can be determined quite accurately throughout the time period that the cloud is included in the photography. With the scale known, the rate of expansion (horizontally and vertically) and drift (at different altitudes) may be approximately determined. As volume is determined by the rate of expansion, indications of the volume could be determined for various times after zero hour.

A preliminary instrument study of this method has been made. Although few measurements were made it is evident that the expansion rate varies throughout the cloud. No complete study has been made of the accuracy that may be achieved but it is believed that about 75 per cent accuracy may be expected.

No factual data on the cloud volume were obtained. Feasibility of use of photogrammetric methods on this type of shot was neither proved nor disproved because of non-synchronization of photograph pairs due to radio signal failure.

3.13 SHOT 13

3.13.1 Edgerton, Germeshausen & Grier Photographic Analysis

Cloud data represented in Figs. 3.43* and 3.43a were computed from camera records collected at Amargosa and Angel's Peak stations. Figure 3.43b was computed from the same records.

3.13.2 Aircraft Reports (See Fig. 3.43)

Sampling aircraft reported the following cloud data: H + 15 min - 40,500 ft top of cloud.

3.13.3 Theodolite Data

Theodolite Location: Control Point
Horizontal Distance to Burst Point: 45,371 ft
Bearing to Burst Point: 341.955°
Burst Height: 4736 ft MSL

3.13.4 Comparison of Cloud Height Observations

Theodolite measurements appear to be erroneous after 7 min compared with the more reliable photographic measurements. This is perhaps due to the edge of the cloud obscuring the actual cloud top which may explain the 8000 ft discrepancy at 14 min.

* Fig. 3.43 curve is constructed as the best fit curve from computed points not indicated on this chart.

3.13.5 Weather Data

Clouds: Clear
Visibility: 15 mi
Weather: None
Shot Height (4736 ft MSL): Temperature, 15.0°C; Pressure, 855 mb; Potential Temperature, 302°K
Pseudo-Adiabatic Chart: See Fig. 3.44
Wind Direction and Speed: See Fig. 3.45

3.13.6 Comparison of Cloud and Weather Data

The cloud behaved very much according to expectations. It penetrated the stratosphere only 2000 ft above the tropopause barrier at 41,000 ft. There were no abrupt shears in the speed and direction of the wind which averaged about 25 knots from 190°. The lapse rate curve was relatively unstable from 6000 to 12,000 ft and again from 19,000 to 25,000 ft which would tend to increase the amount of rise.

3.14 SHOT 14

3.14.1 Edgerton, Germeshausen & Grier Photographic Analysis

The cloud data indicated in Fig. 3.46* and 3.46a were computed from camera records collected at Amargosa and Angel's Peak. Figure 3.46b was computed from the same records.

3.14.2 Aircraft Reports (See Fig. 3.46)

Sampling aircraft reported the following cloud data: H + 15 min - 37,200 ft top of cloud.

3.14.3 Theodolite Data

Theodolite Location: Control Point
Horizontal Distance to Burst Point: 59,024 ft
Bearing to Burst Point: 8.735°
Burst Height: 4745 ft

3.14.4 Comparison of Cloud Height Observations

Photographic and theodolite measurements agree quite well through 5 min after which time only essential features agree such as a sinking of cloud at 7 min followed by a slight rise. However, the maximum heights reached differ by about 5000 ft suggesting once more the dubious reliability of theodolite measurements.

* Fig. 3.46 curve is constructed as the best fit curve from computed points not indicated on this chart.

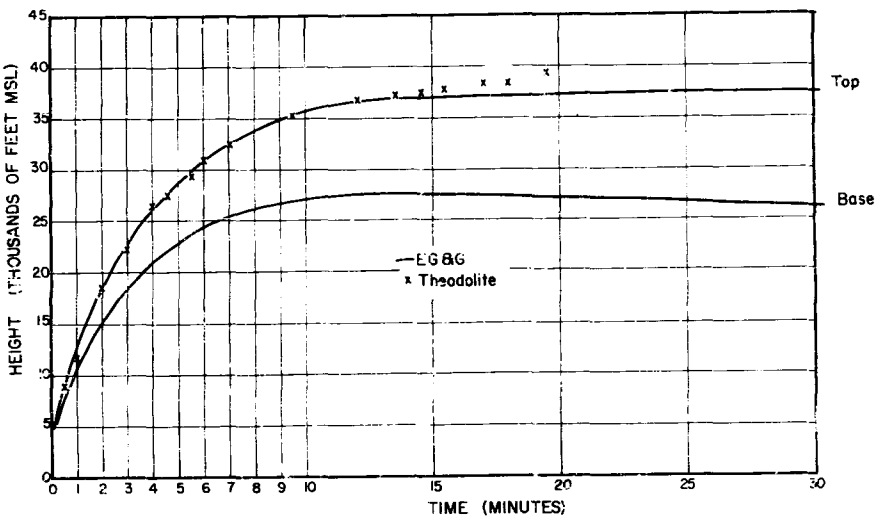

Fig. 3.14 Cloud Rise vs Time, Shot 5

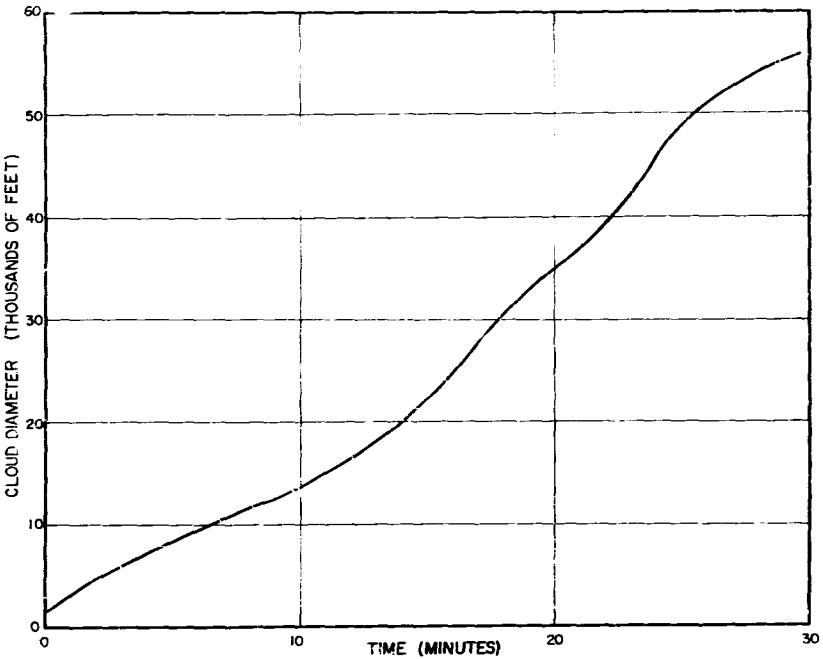

Fig. 3.14a Cloud Diameter vs Time, Shot 5 (EG&G Analysis)

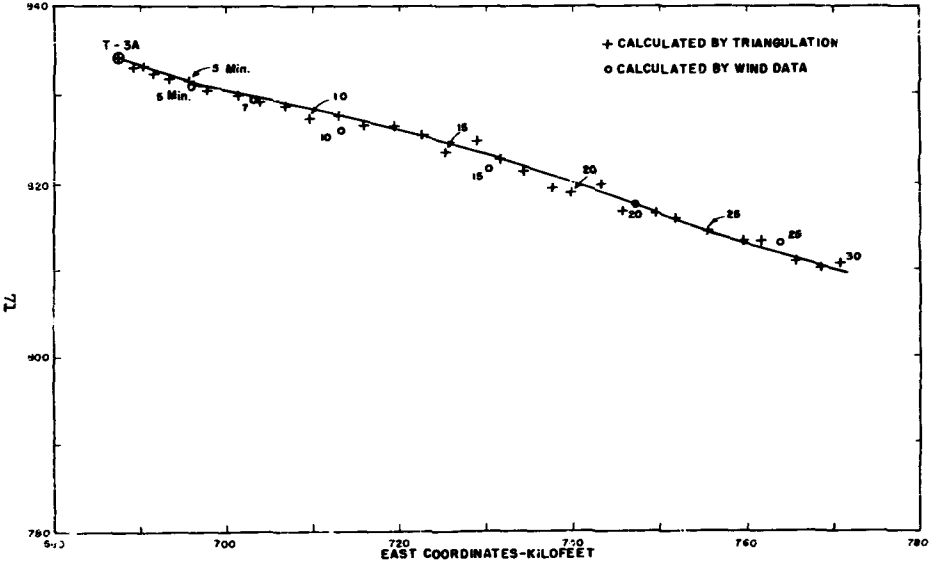

Fig. 3.14b Cloud Drift, Shot 5 (EG&G Analysis)

3.14.5 Weather Data

Clouds: Clear
Visibility: 15 mi
Weather: None
Shot Height (4745 ft MSL): Temperature, 2.1°C; Pressure, 851 mb; Potential Temperature, 282°K
Pseudo-Adiabatic Chart: See Fig. 3.47
Wind Direction and Speed: See Fig. 3.48

3.14.6 Comparison of Cloud and Weather Data

The height predicted for this cloud was overestimated by 2000 ft. This error can perhaps be attributed to the stable layer between 20,000 and 27,000 ft which was coincident with a strong vertical shear in the wind speed. Also, a shallow inversion existed at 34,000 to 35,000 ft. Both of these features would tend to hinder the cloud rise. The cloud stopped rising in the middle of a thick layer of strong (65-70 knots) westerly winds. The lapse rate curve was stable throughout the cloud's vertical trajectory.

TABLE 3.13 - Theodolite Data, Shot 13

Time (min)	Elevation Angle	Horizontal Distance (ft)	Cloud Height (ft MSL)
0.0	-	45,371	4,736
0.65	11.3	45,930	13,305
1.0	16.1	46,810	17,635
1.5	20.6	48,240	22,240
2.0	23.3	49,450	25,400
2.5	25.9	50,320	28,540
3.0	27.9	51,080	31,160
3.5	29.9	51,740	33,880
4.0	31.0	52,320	35,570
4.5	32.1	53,100	37,440
5.0	32.9	53,900	39,010
5.5	34.2	54,830	41,410
6.0	34.6	55,900	42,660
6.5	34.8	56,950	43,690
7.0	34.9	58,000	44,630
7.5	35.0	59,200	45,610
8.5	35.3	61,500	47,730
9.5	34.7	64,000	48,430
10.0	34.2	65,320	48,490
10.5	34.0	66,700	49,080
11.0	33.6	68,050	49,330
11.5	33.3	69,450	49,780
12.0	32.8	70,800	49,810
12.5	32.7	72,240	50,480
14.0	31.5	76,500	51,030

TABLE 3.14 - Theodolite Data, Shot 14

Time (min)	Elevation Angle	Horizontal Distance (ft)	Cloud Height (ft MSL)
0.0	-	59,024	4,745
0.5	7.7	58,650	11,960
1.0	12.85	57,800	17,330
1.5	17.1	57,330	21,760
2.0	20.8	58,000	26,180
2.5	23.4	59,500	29,880
3.0	25.5	61,050	33,240
3.5	26.7	62,800	35,710
4.0	27.1	65,100	37,420
4.5	27.1	67,400	38,580
5.0	26.6	69,550	38,930
5.5	26.5	71,800	39,930
7.0	23.7	79,600	39,110
7.5	23.3	82,200	39,530
8.0	22.5	85,150	39,390
8.5	22.6	87,750	40,590
9.0	22.0	90,250	40,630
9.5	21.5	93,200	40,810
10.0	21.0	95,300	40,720
10.5	20.5	98,000	40,730
11.0	20.1	100,800	41,030
11.5	19.4	103,250	40,530
12.0	19.0	106,000	40,680
12.5	18.7	108,800	40,930

3.15 APPLICATION OF CLOUD DATA TO PRESENT PREDICTION METHODS

The consolidated data of this series were applied to the Sutton and Taylor equations of Table 1.1 and solutions were obtained for the yield parameter. Computations were made independently using the maximum rise of both cloud centers and cloud tops for the height parameter. The results are illustrated in Figs. 3.50 and 3.50a and also in Fig. 3.50b in the form of percentage error in computed yields, where assigned yields (adjusted to MSL) were assumed correct. It is evident in Fig. 3.50b that Shot 5 presents a special case for reasons not yet determined. The initial height prediction for this shot was 10,000 ft too low. The following general statements do not take this shot into consideration. None of the equations succeeded in systematically predicting the yield with acceptable accuracy. The use of maximum rise of cloud centers for the height parameter produced the best results but verified only within approximately a factor of two. Both versions of the Taylor equation achieved this limited accuracy whereas only Sutton's vertical rise equation did as well.

TABLE 3.15 - Computed Potential Temperature Excess ($\Delta\theta_o$) for TEAPOT Shots (at moment when cloud begins to rise)

Shot	Yield		Computed $\Delta\theta_o$ (°C) using a height parameter equal to the amount of rise of cloud	
	Assigned	Adjusted to MSL	Center	Top
1	1.2	1.4	42	66
2	2.5	2.9	113	217
3	7.0	8.2	192	547
4	43.0	51.0	1736	3645
5	3.6	4.2	580	1189
6	8.4	9.9	612	1370
7	1.2	1.4	*	*
8	15.5	17.9	183	388
9	3.1	3.7	*	*
10	3.1	14.3	407	407
11	1.5	1.8	38	53
12	24.0	27.6	723	1760
13	30.0	35.6	1201	2402
14	28.0	33.4	587	1375

*Data insufficient or unsuitable for computation.

The Machta equation was used to determine representative potential temperature excesses existing in atomic clouds at the moment the cloud as a whole begins to rise. The assumption of a constant mass entrainment value of $0.5 \times 10^{-3} m^{-1}$ was made for $\partial M/M\partial z$. Again, the computations were made independently using the amount of rise for both cloud centers and cloud tops as the height parameter. The results shown in Table 3.15 do not reflect the desired direct relationship with yield. Whether or not the values shown represent the true picture cannot be ascertained because actual values for the temperature excess of atomic clouds have not been recorded thus far.

With the exception of Shots 7 and 9, when data were insufficient or unsuitable for computation, an attempt was made to determine the character of volume entrainment $\partial V/V\partial z$ as the cloud rises. The crude assumption was made that the atomic cloud maintained the general shape of an oblate spheroid throughout its evolution. The EG&G cloud data enabled us to compute volumes as shown in Fig. 3.51. The cloud associated with Shot 10 was a circular torus ring, however, EG&G data indicate that a cross-section of the ring had an elliptical shape. In this case, the volume was determined accordingly and hence the volume computations should be more representative than that of the other shots. The role played by moisture advection (through entrainment) in determining the apparent size of the cloud is brought into focus by the curve for Shot 10 where moisture was relatively absent. Otherwise, the volume seems to be a function of yield in general, as expected. Values of volume entrainment were then computed and plotted against height of cloud center in Fig. 3.52. Only values for Shots 3, 4, 5, 6, 8, 12, 13, and 14 are shown in the graph because other shots were of too low a yield to produce a great enough height range between burst and stabilization to establish a definite trend. The curve for Shot 4 is omitted for the sake of clarity but is very similar to that for Shot 13. The volume entrainment for Shot 10 was negative after 0.5 min and is not shown in the graph. The overall results are in good agreement with previous work along these line. 14/ One, therefore, seems quite justified in assuming that volume entrainment is insensitive to yield and relatively constant at a value of $0.5 \times 10^{-3} m^{-1}$ between approximately 15,00 and 35,000 ft.

As a final step, a comparison was made of the various prediction methods other than by the use of the dynamic equations of Table 1.1. A tabulation of the results appears in Table 3.1f. The surprising feature of this table is that Column 5, and not Columns 7 or 9, as one should expect, produced the best results. This situation points out the great need for further refinement of the regression equation to render it more suitable for operational use. Perhaps the equation should encompass more parameters, e.g., moisture content of the ambient atmosphere. Also, departures from standard conditions, in each case considered, may be a better measure of the atmosphere's influence upon cloud rise than the present scheme of using absolute values.

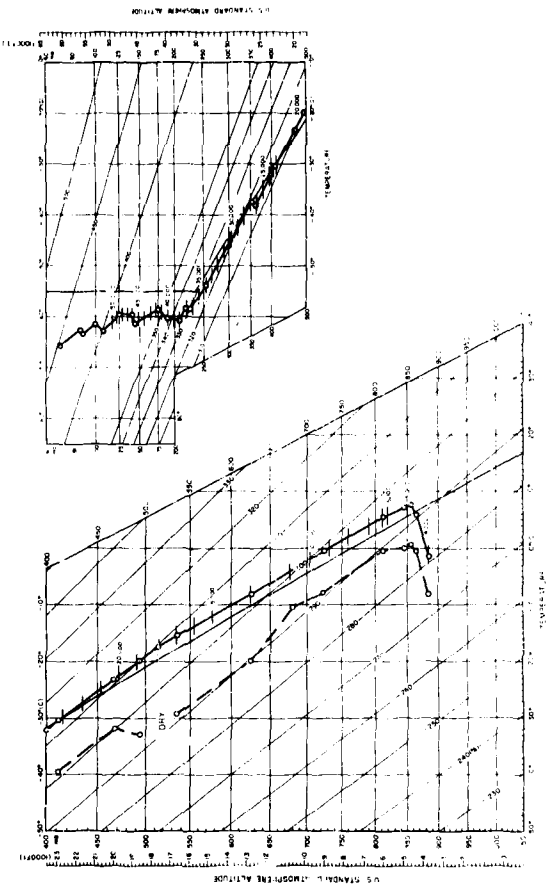

Fig. 3.15 Pseudo-Adiabatic Chart, Shot 5

TABLE 3.16 – Comparison of Height Prediction Methods

Shot	Yield			Predicted Maximum Heights (1000's of Ft MSL) Based From Various Methods											
1	2	3	4	5	6	7	8	9	10	11	12	13	14		
	Assigned	Adjusted to HSL	Most plausible maximum height observed (1000's ft MSL) (Derived from three sources of data)	Regression equation and Forecast data (Computed at test site)	Error	Regression equation and actual data (Computed by LASL)	Error	Regression equation and actual data (Computed by Weather Bureau)	Error	Amount of rise vs yield curve for past data and actual yield	Error	Assumption of fixed maximum height for yields of 15–60 KT	Error		
1	1.2	1.4	20	24		24	4.0	26.5	6.5	15.5	4.5				
2	2.5	2.9	24.5		0.5	26	1.5	26.5	2.0	20.5	4.0				
3	7.0	8.2	30	26	4.0	28	2.0	28.0	2.0	31.0	1.0				
4	43.0	51.0	45	43	2.0	46	1.0	47.0	2.0	41.5	3.5				
5	3.6	4.2	37	38	1.0	29	9.0	22.5	14.5	24.0	13.0				
6	8.4	9.9	39.5	35–40	2.0	29	10.5	36.0	3.5	33.0	3.5				
7	1.2	1.4	12	8–10*						38.5	1.5				
8	15.5	17.9	22	29	7.0	49	17.0	49.5	17.5	38.5	6.5				
9	3.1	3.7	34.5	36		36	5.5	32.5	1.0	29.5	8.0				
10	3.1	14.3	35	(Not applicable)											
11	1.5	1.8	15.5	24	8.5	25	0.5	15.5	0.0	17.0	1.5				
12	24.0	27.6	43.5	39	2.5	39	2.5	36.5	6.0	39.5	2.0				
13	33.0	38.6	43	42	1.0	45	2.0	47.5	4.0	41.5	1.5				
14	28.0	33.4	36	38	2.0	35	1.0	40.0	4.0	41.0	5.0				
Mean of absolute error				3.65		4.71		5.25		4.50				4.30	
Prediction is generally				Too low		Too low		Too high		Too low				Too low	

*Prediction made by means other than regression equation.

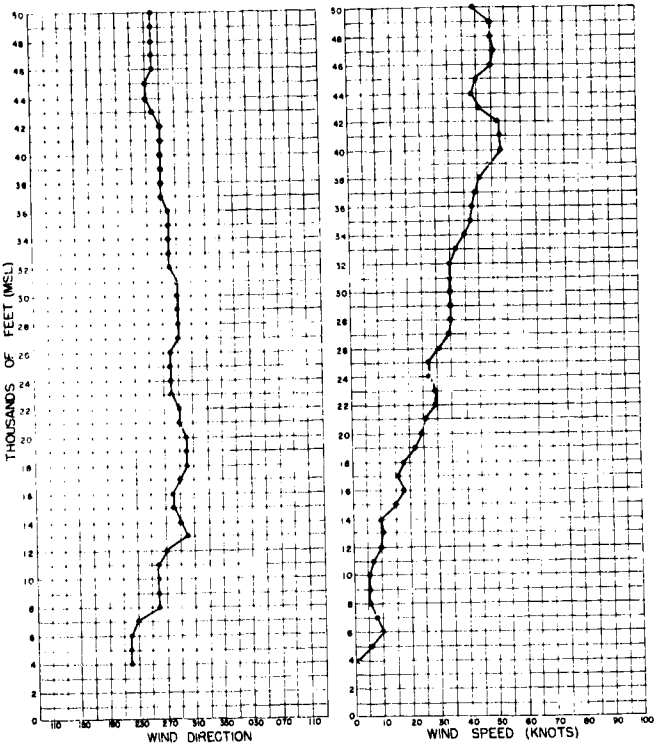

Fig. 3.16 Wind Speed and Direction, Shot 5

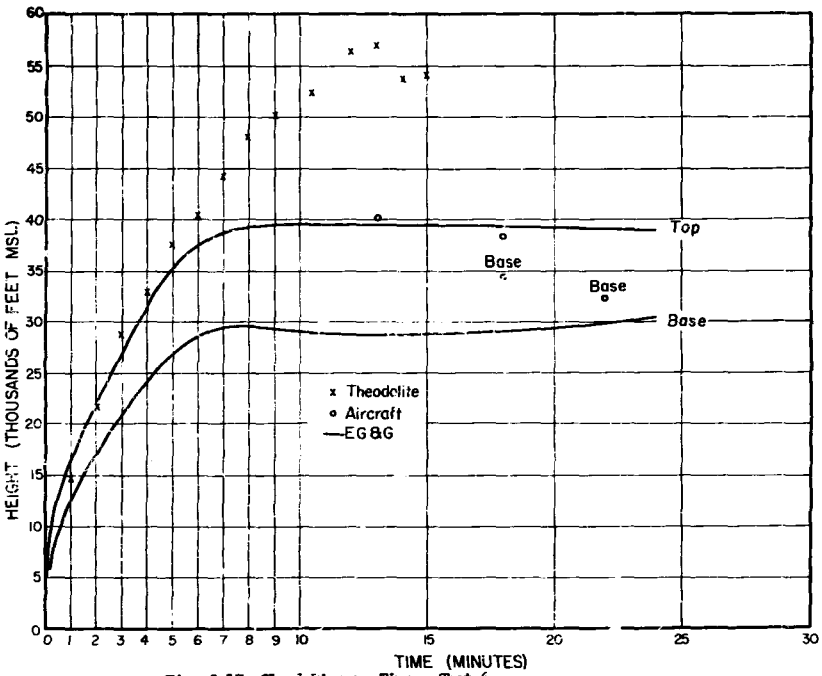

Fig. 3.17 Cloud Rise vs Time, Shot 6

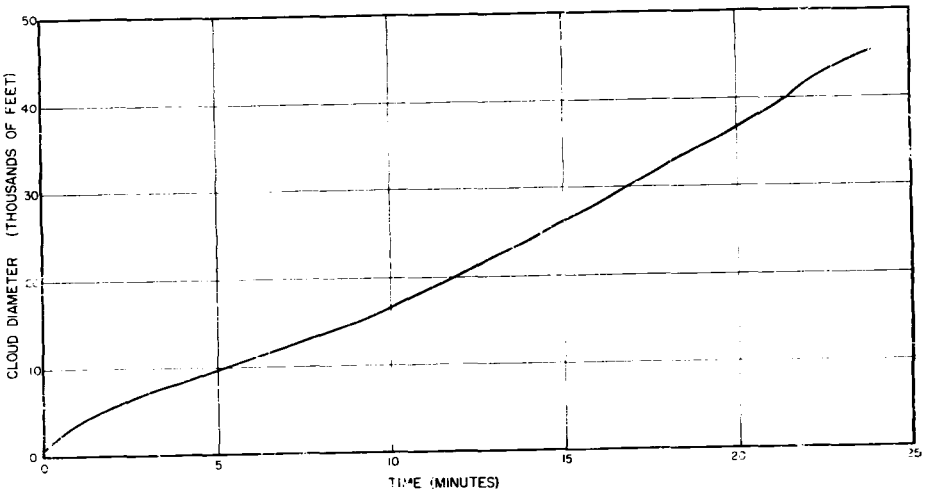

Fig. 3.17a Cloud Diameter vs Time, Shot 6 (EG&G Analysis)

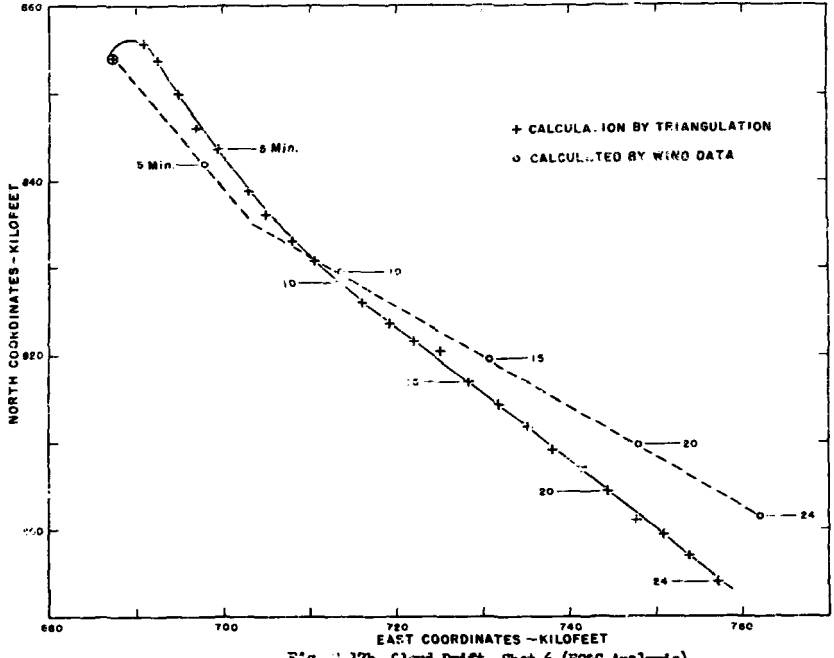

Fig. 3.17b Cloud Drift, Shot 6 (EG&G Analysis)

Fig. 3.13 Pseudo-Adiabatic Chart, Shot 6

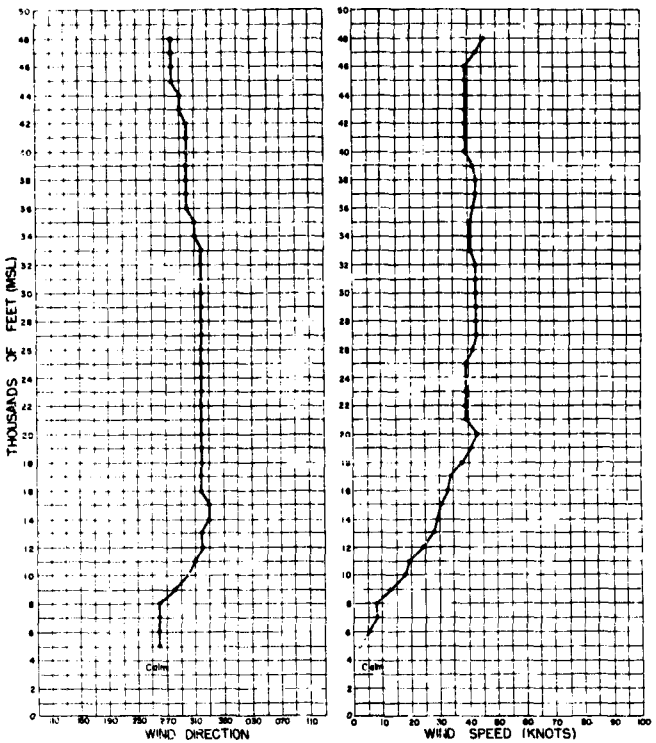

Fig. 3.19 Wind Speed and Direction, Shot 6

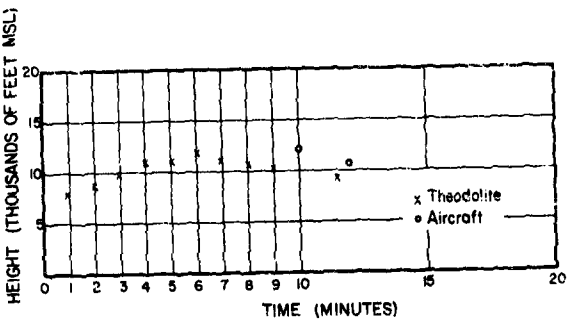

Fig. 3.20 Cloud Rise vs Time, Shot 7

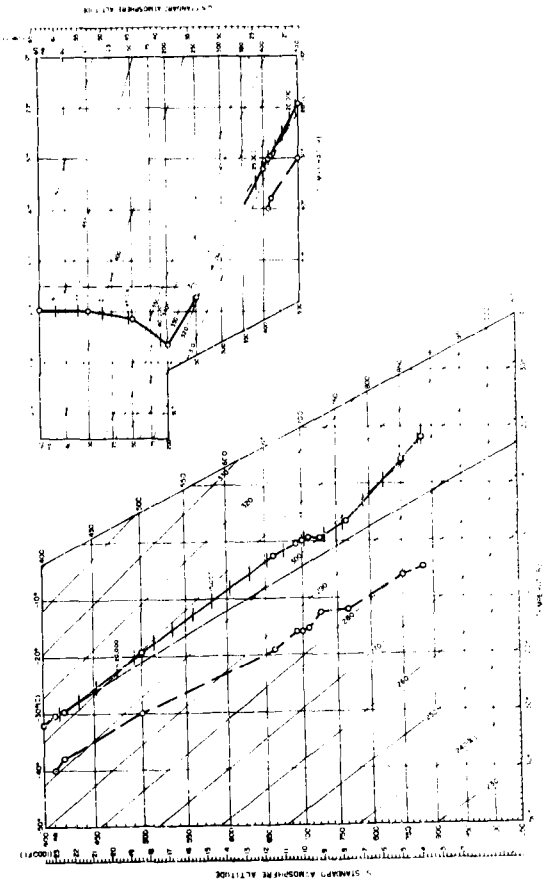

Fig. 3.21 Pseudo-Adiabatic Chart, Shot 7

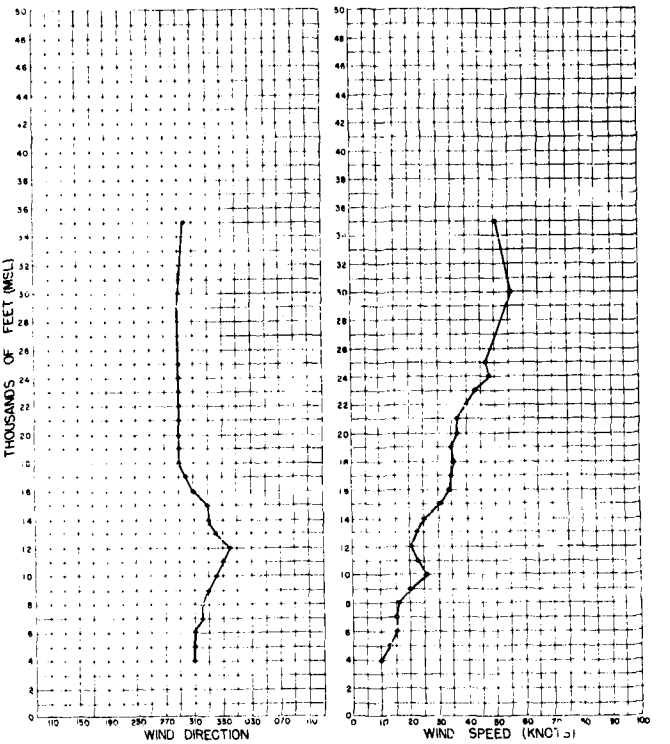

Fig. 3.22 Wind Speed and Direction, Shot 7

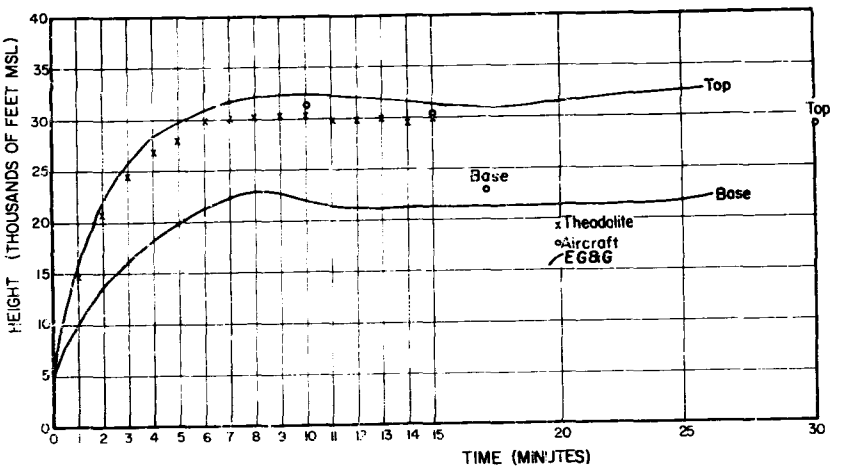

Fig. 3.23 Cloud Rise vs Time, Shot 5

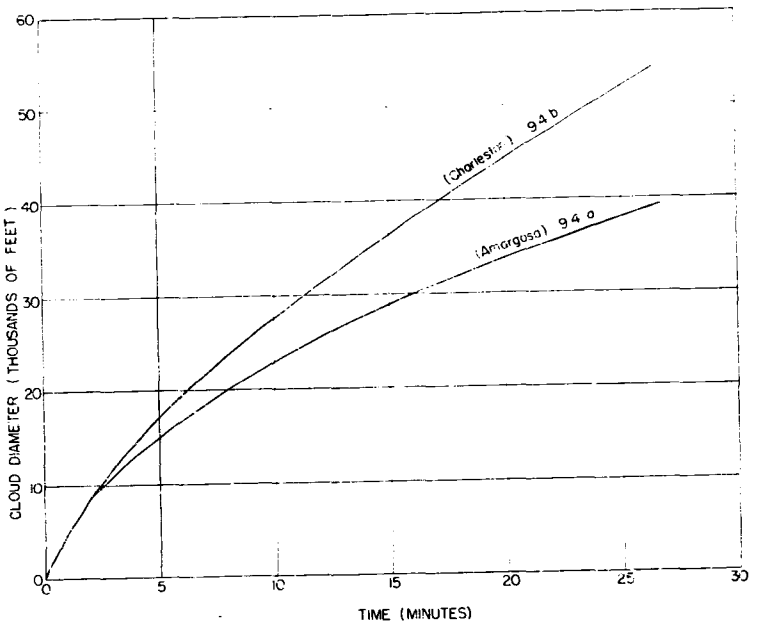

Fig. 3.23a Cloud Diameter vs Time, Shot 8 (EG&G Analysis)

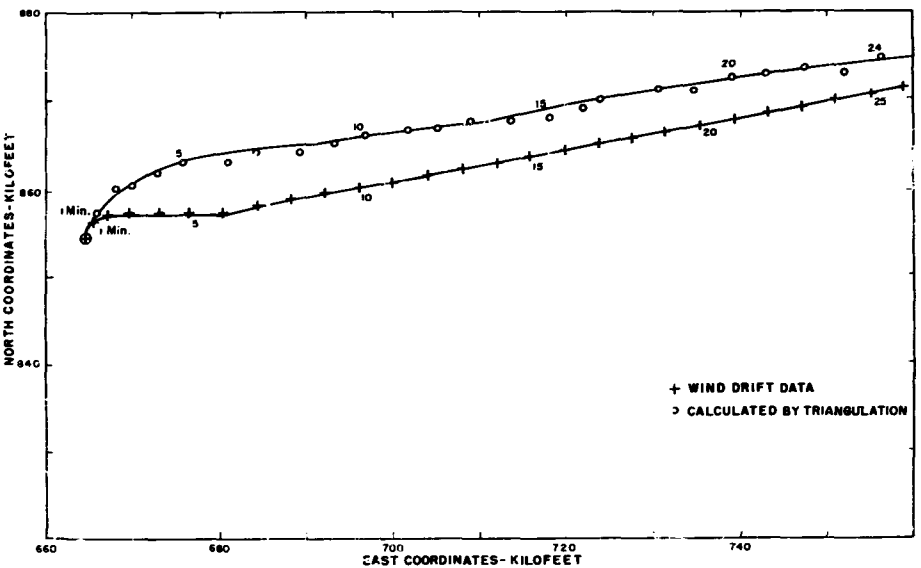

Fig. 3.23b Cloud Drift, Shot 8 (EG&G Analysis)

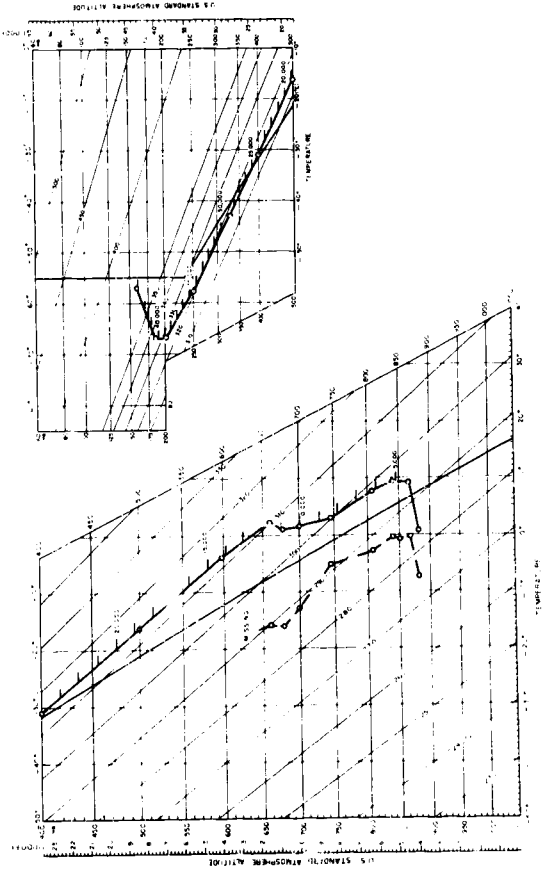

Fig. 3.24 Pseudo-Adiabatic Chart, Shot 8

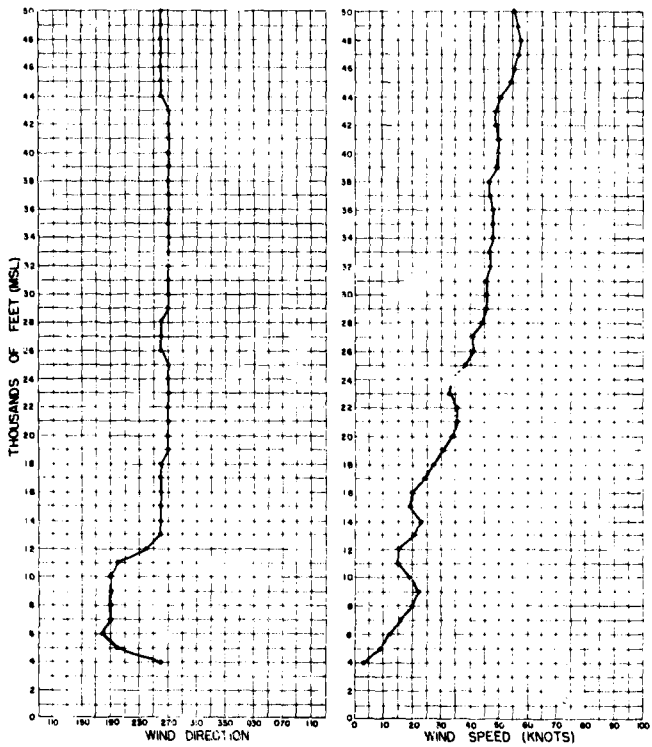

Fig. 3.25 Wind Speed and Direction, Shot 3

Fig. 3.26a Shot 7 Cloud (approx H + 7 Sec). Note jets.

Fig. 3.26b Shot 8 Cloud (approx H + 1 Min).
Note bomb light surrounding mushroom.

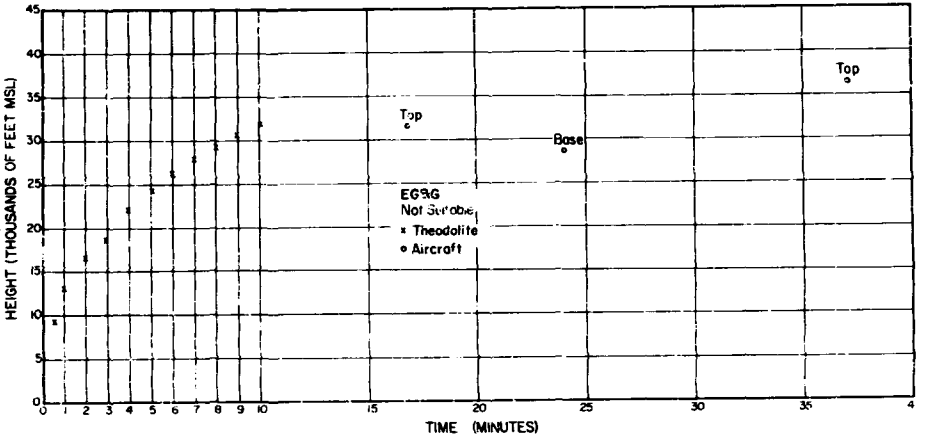

Fig. 3.27 Cloud Rise vs Time, Shot 9

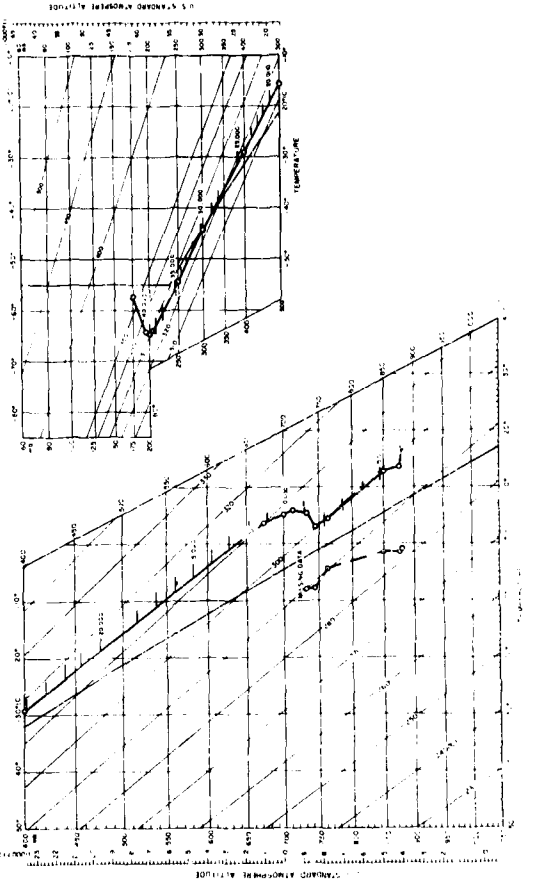

Fig. 3.22 Pseudo-Adiabatic Chart, Shot 9

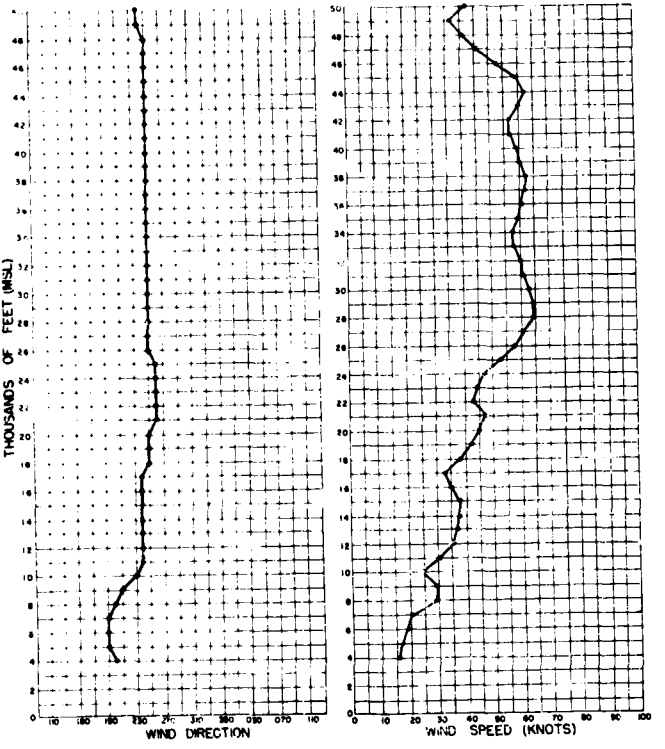

Fig. 3.29 Wind Speed and Direction, Shot 9

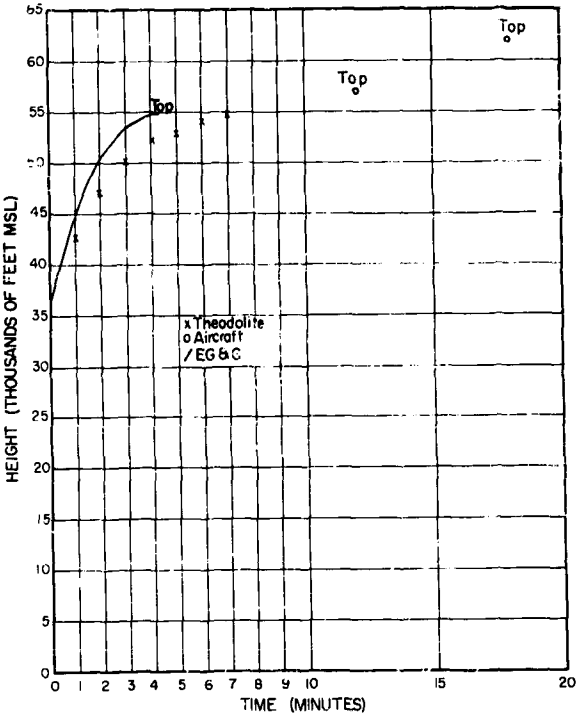

Fig. 3.30 Cloud Rise vs Time, Shot 10

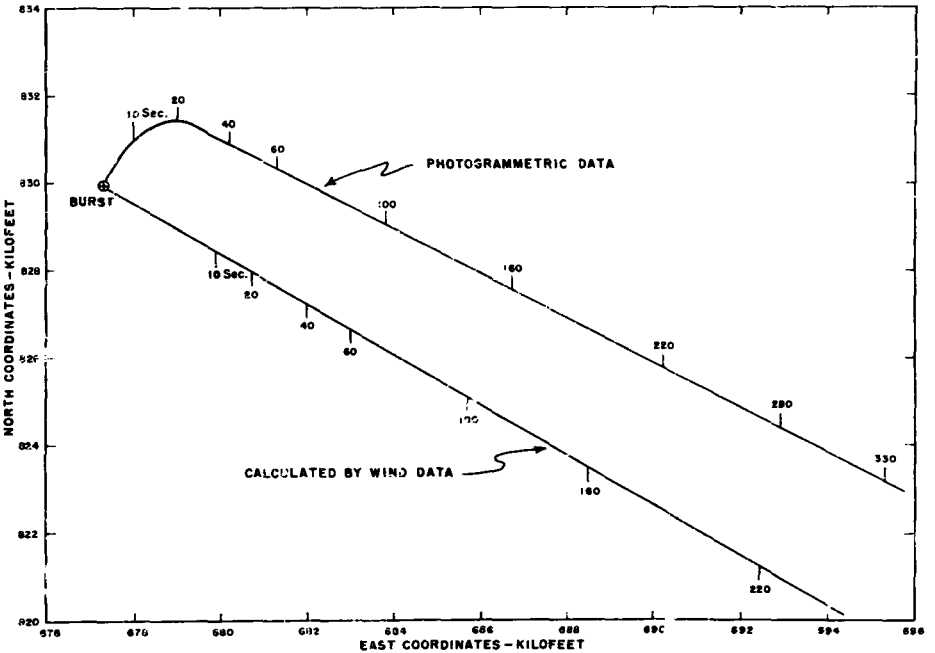

Fig. 3.30b Cloud Drift, Shot 10 (EG&G Analysis)

Fig. 3.3Ce Vertical Thickness vs Time, Shot 10 (SSSG Analysis)

Fig. 5.31 Pseudo-Adiabatic Chart, Shot 10

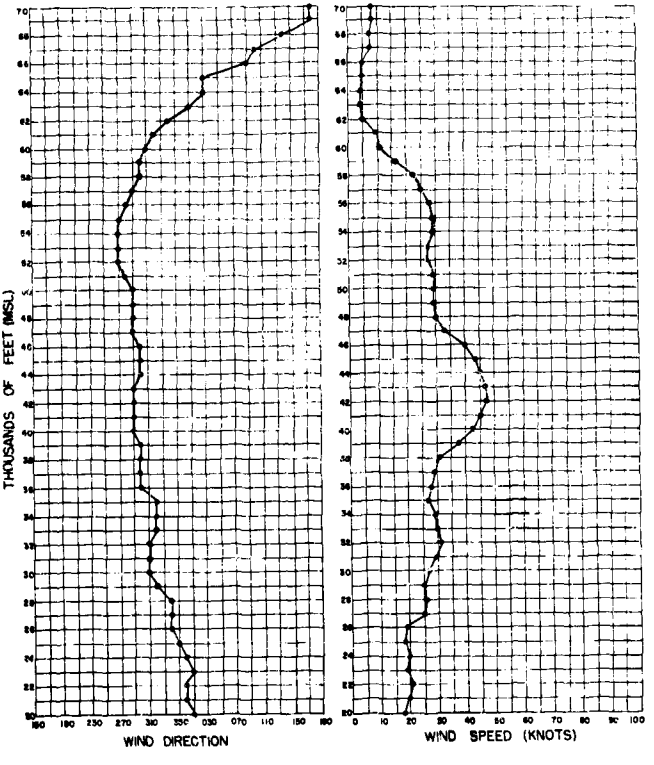

Fig. 3.32 Wind Speed and Direction, Shot 10

Fig. 3.33a Shot 9 Cloud (approx H + 12 sec)

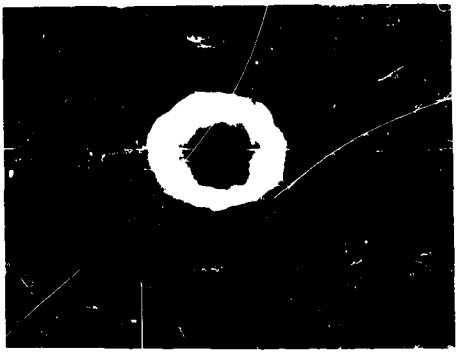

Fig. 3.33b Shot 10 Cloud (approx H + 1 min)

Fig. 3.33c Shot 10 Cloud (approx H + 15 sec). Note lack of density of ring.

Fig. 3.33d Shot 10 Cloud (approx H + 90 sec). Note lack of density of ring.

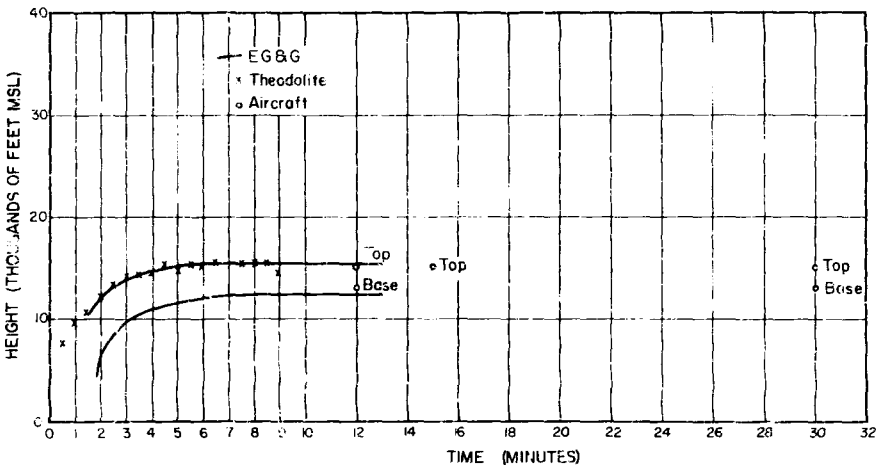

Fig. 3.34 Cloud Rise vs Time, Shot 11

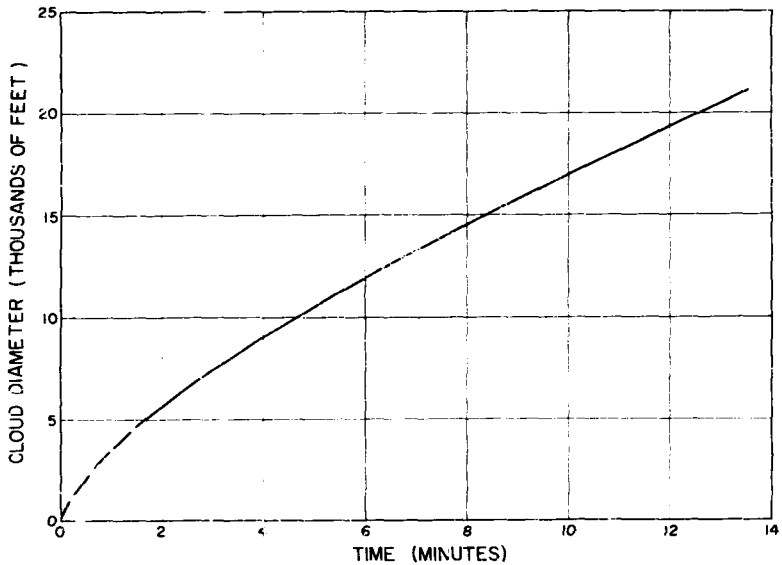

Fig. 3.34a Cloud Diameter vs Time, Shot 11

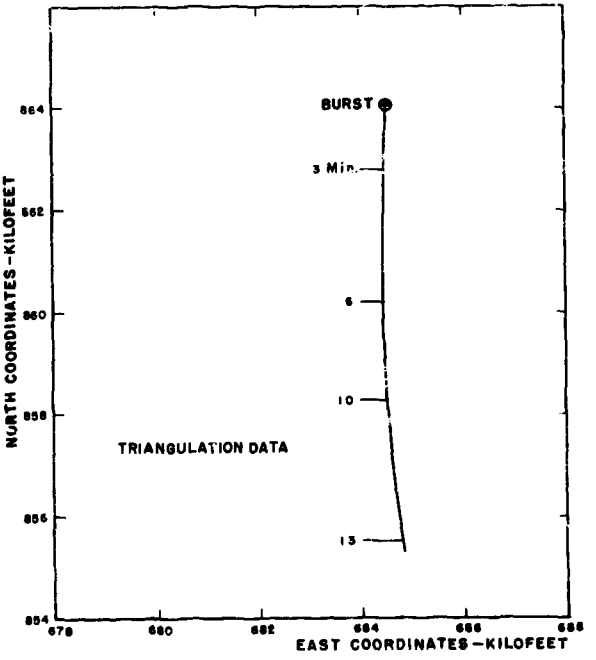

Fig. 3.34b Cloud Drift, Shot 11 (EG&G Analysis)

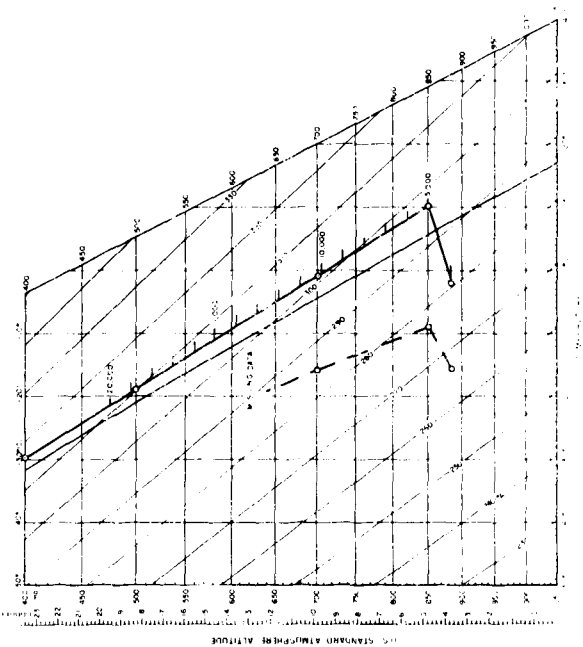

Fig. 3.15 Pseudo-adiabatic Chart, Shot II

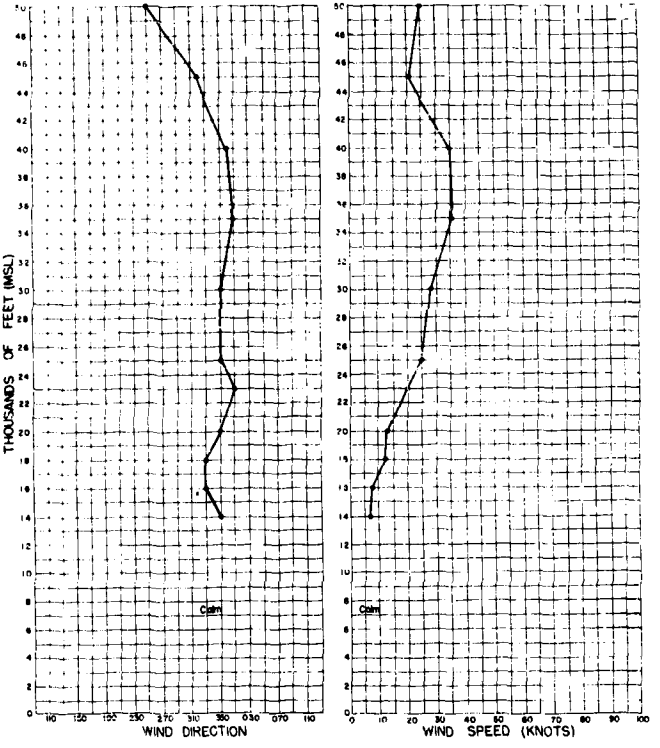

Fig. 3.3b Wind Speed and Direction, Shot 11

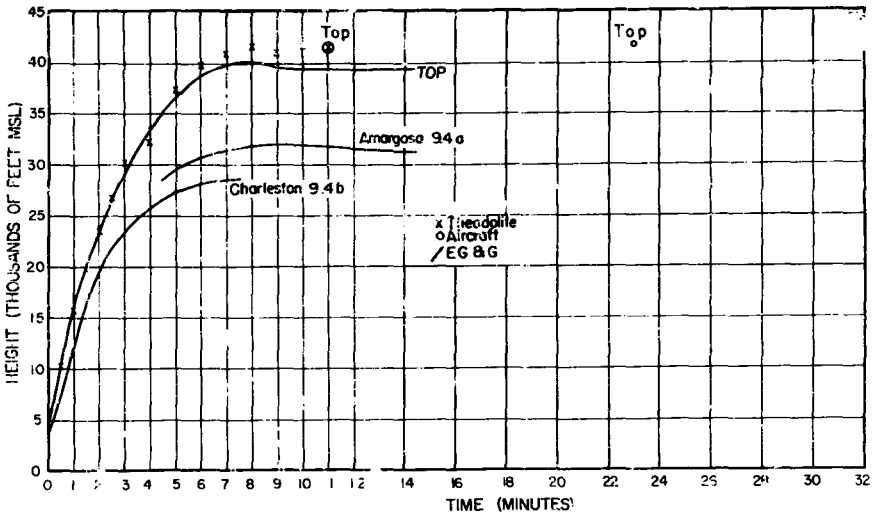

Fig. 3.37 Cloud Rise vs Time, Shot 12

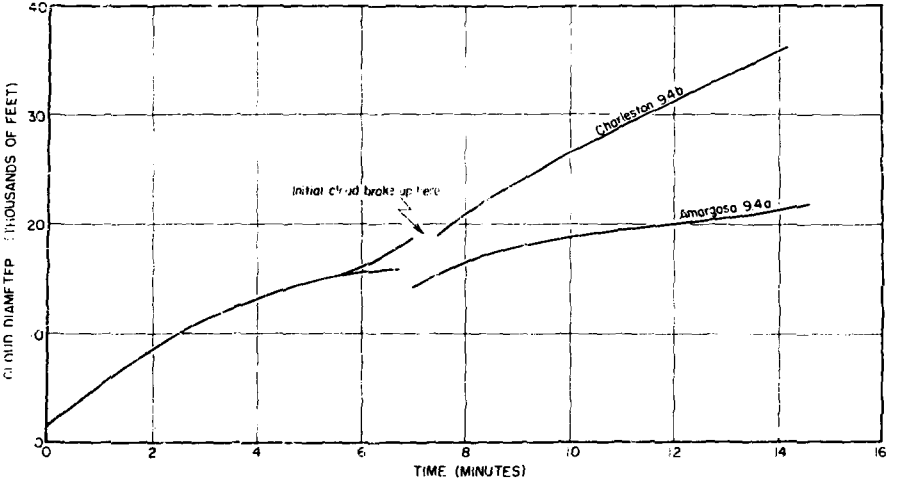

Fig. 3.37a Cloud Diameter vs Time, Shot 12

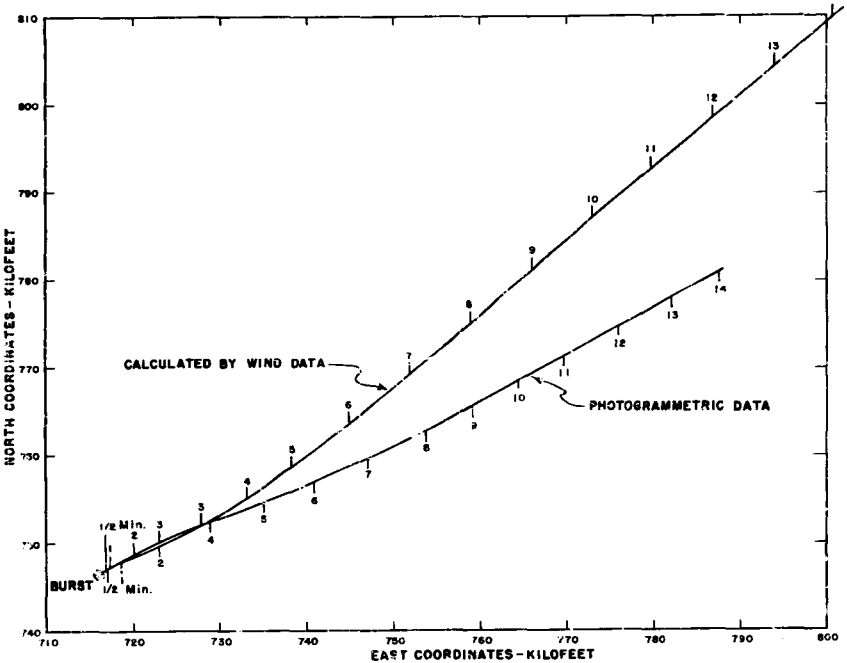

Fig 3.37b Cloud Drift, Shot 12

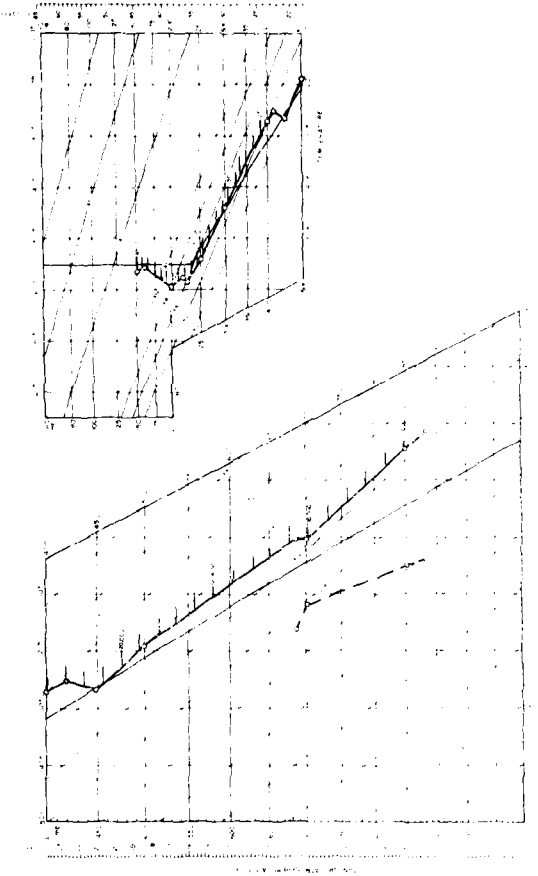

Fig. 3.36 Pseudo-Adiabatic Chart, Shot 12

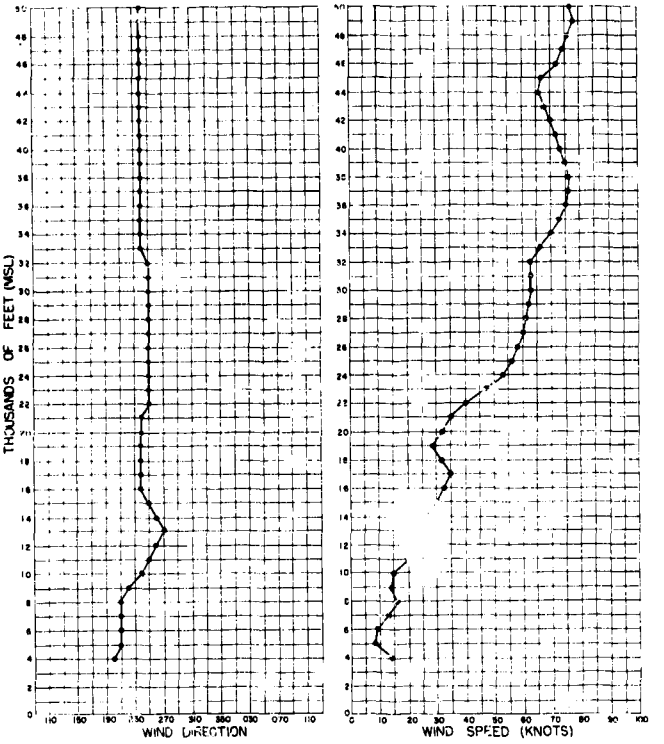

Fig. 3.39 Wind Speed and Direction, Shot 12

Fig. 3.40 Shot 12 Cloud (approx H + 15 sec). Note good cloud definition.

Fig. 3.41 Shot 12 Cloud (approx H + 200 sec). Note good cloud definition.

Fig. 3.42a Shot 12 Cloud (approx H + 31 sec). Photo taken from 42,000 ft above burst with a KA-3 camera.

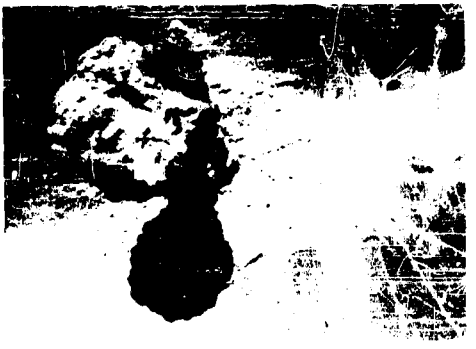

Fig. 3.42b Shot 12 Cloud (approx H + 42 sec). Photo taken from 42,000 ft above burst with a KA-3 camera.

Fig. 3.42c Shot 12 Cloud (approx H + 46 sec). Photo taken from 42,000 ft above burst with a KA-3 camera.

Fig. 3.42d Shot 12 Cloud (approx H + 54 sec). Photo taken from 42,000 ft above burst with a KA-3 camera.

Fig. 3.42e Shot 13 Cloud (approx H + 6 sec). Photo taken from 42,000 ft above burst with a KA-3 camera mounted vertically on aircraft.

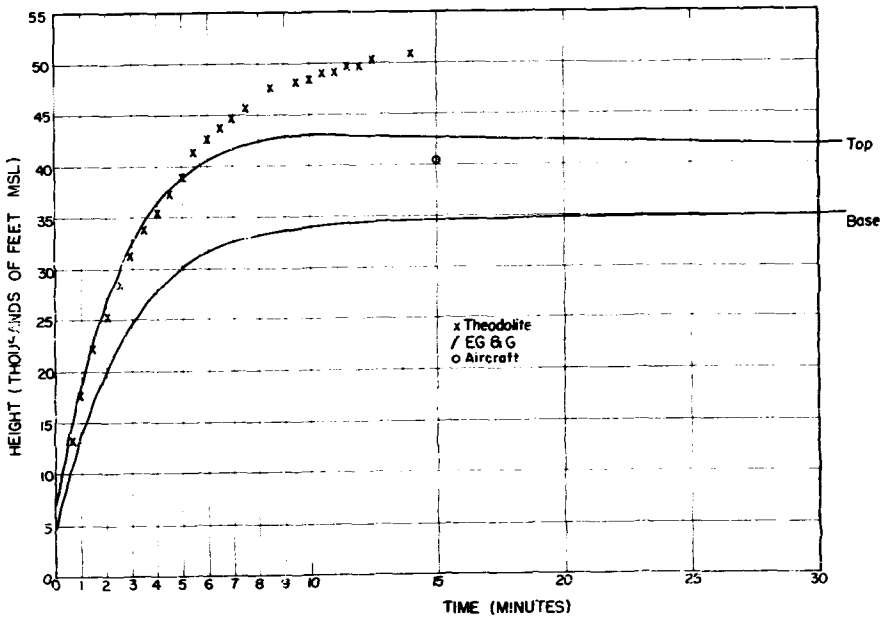

Fig. 3.43 Cloud Rise vs Time, Shot 13

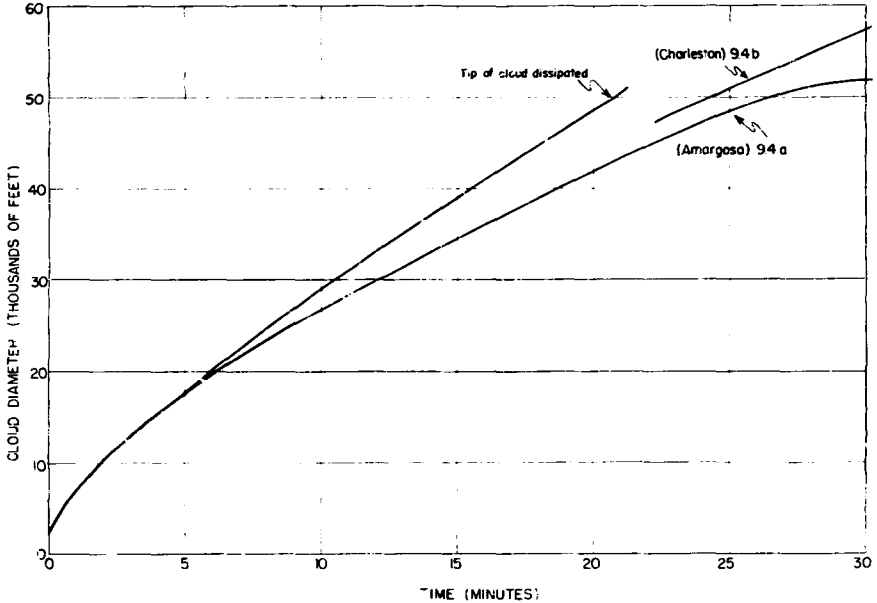

Fig. 3.43a Cloud Diameter vs Time, Shot 13 (EG&G Analysis)

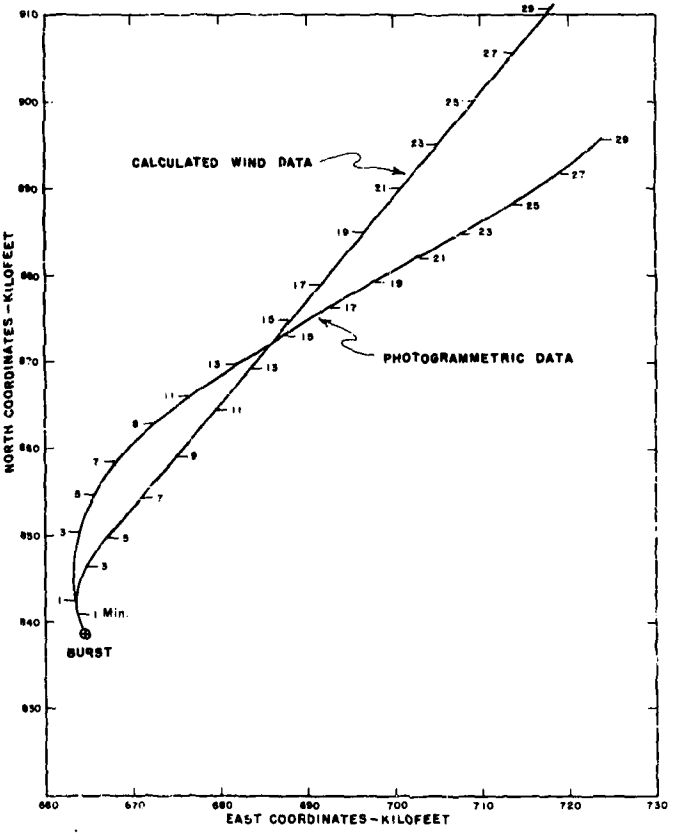

Fig. 3.43b Cloud Drift, Shot 13 (EG&G Analysis)

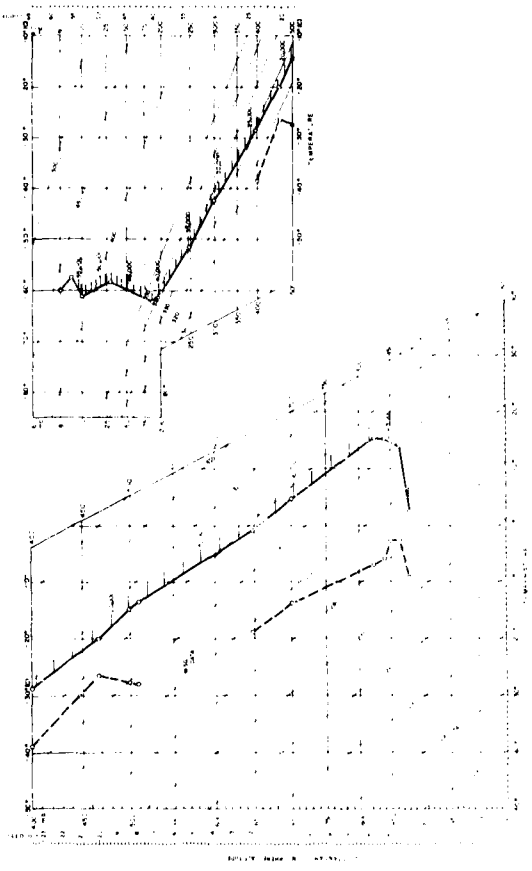

Fig. 3.44 Pseudo-adiabatic Chart, Shot 13

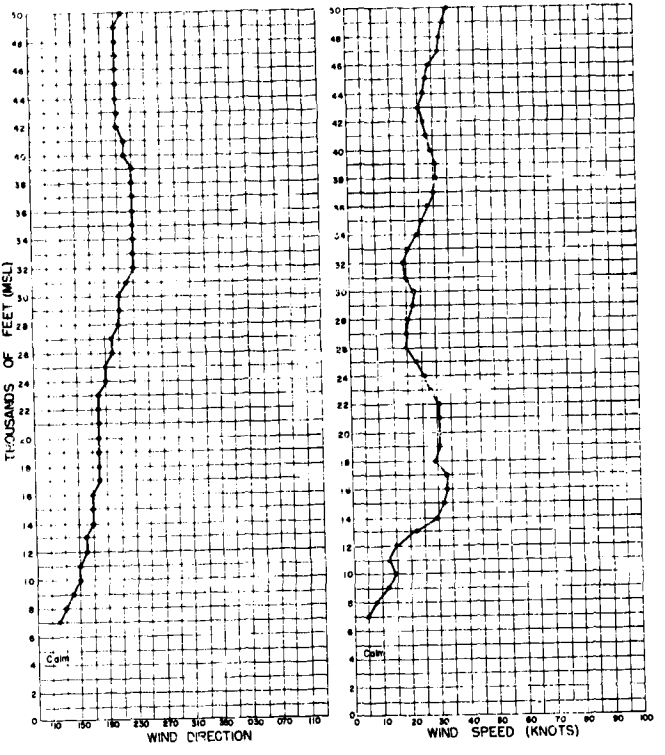

Fig. 3.45 Wind Speed and Direction, Shot 13

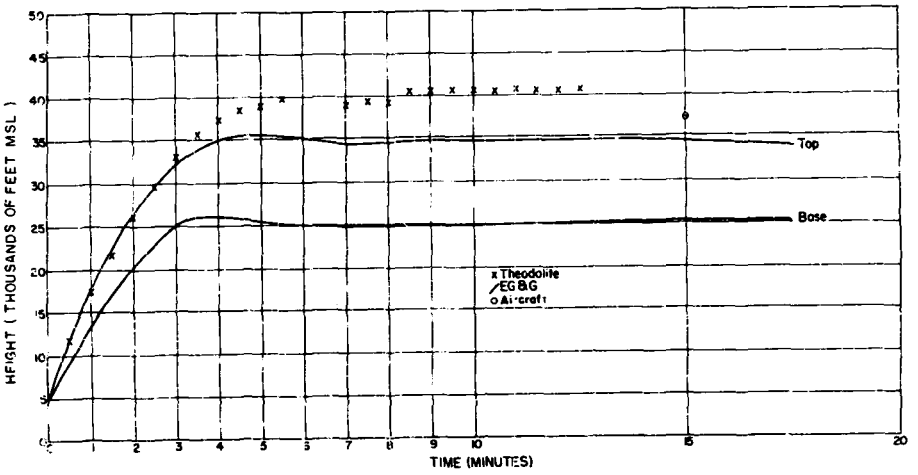

Fig. 3.46 Cloud Rise vs Time, Shot 14

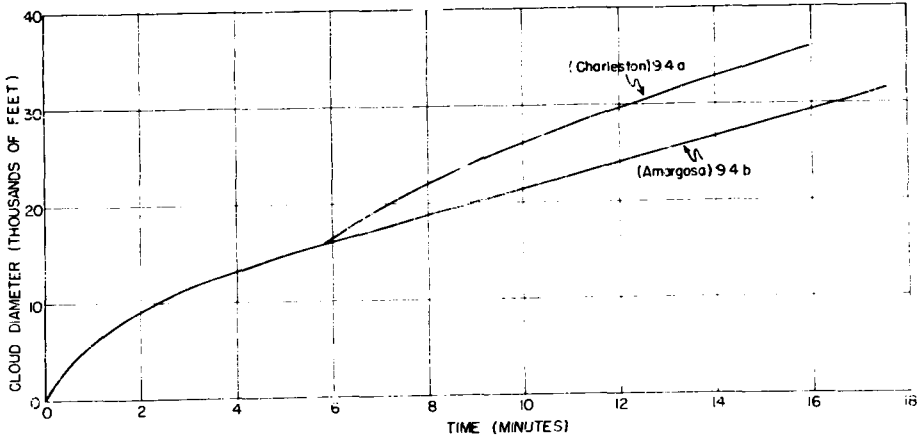

Fig. 3.46a Cloud Diameter vs Time, Shot 14 (EG&G Analysis)

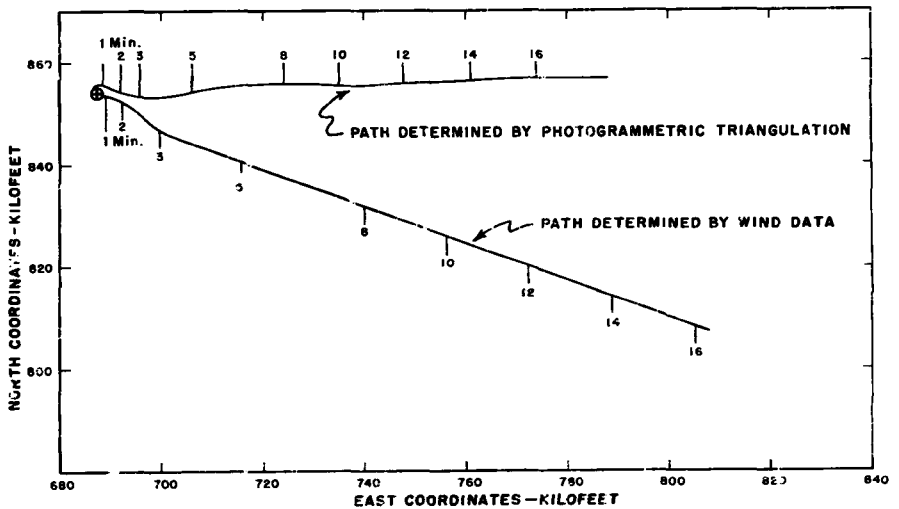

Fig. 3.466 Cloud Drift, Shot 14 (EG&G Analysis)

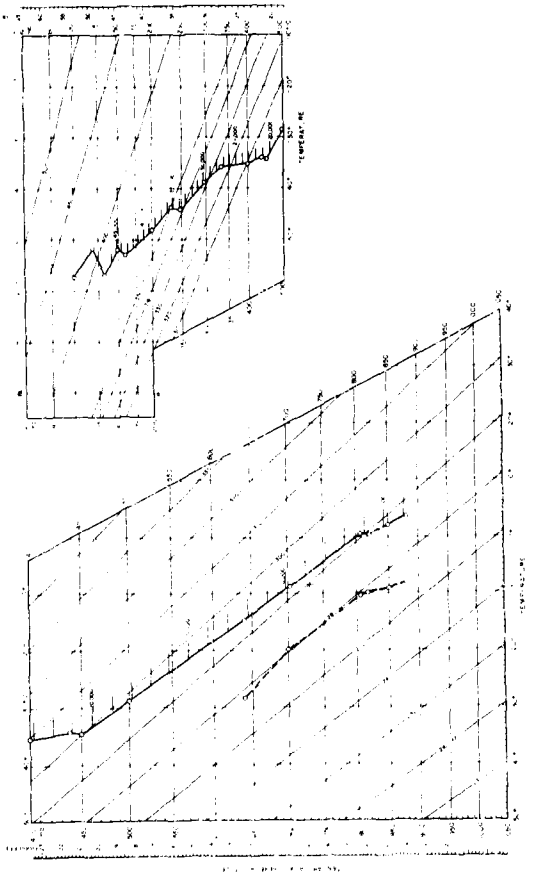

Fig. 3.47 Pseudo-Adiabatic Chart, Shot 14

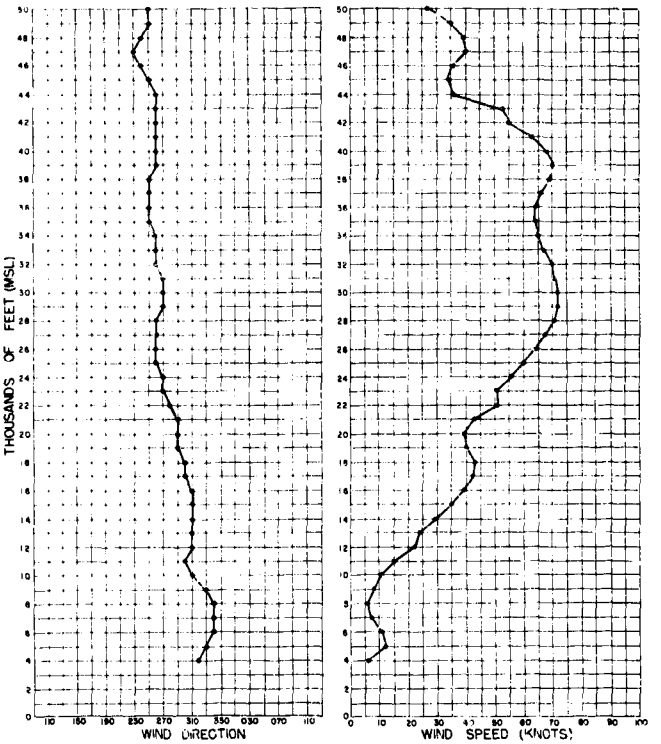

Fig. 3.48 Wind Speed and Direction, Shot 14

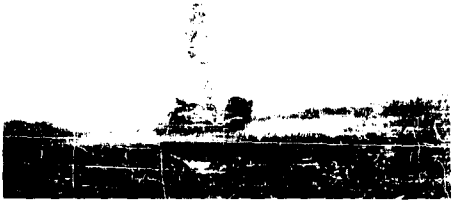

Fig. 3.49 Shot 14 Cloud (approx 11 + 1 min). Note non uniformity of stem and residual lip to mushroom.

Fig. 3.5 Actual Yields vs Computed Yields – Using Vertical Size Concept

Fig. 3.50a Actual Yield vs Computed Yield - Using Accuracy Concept

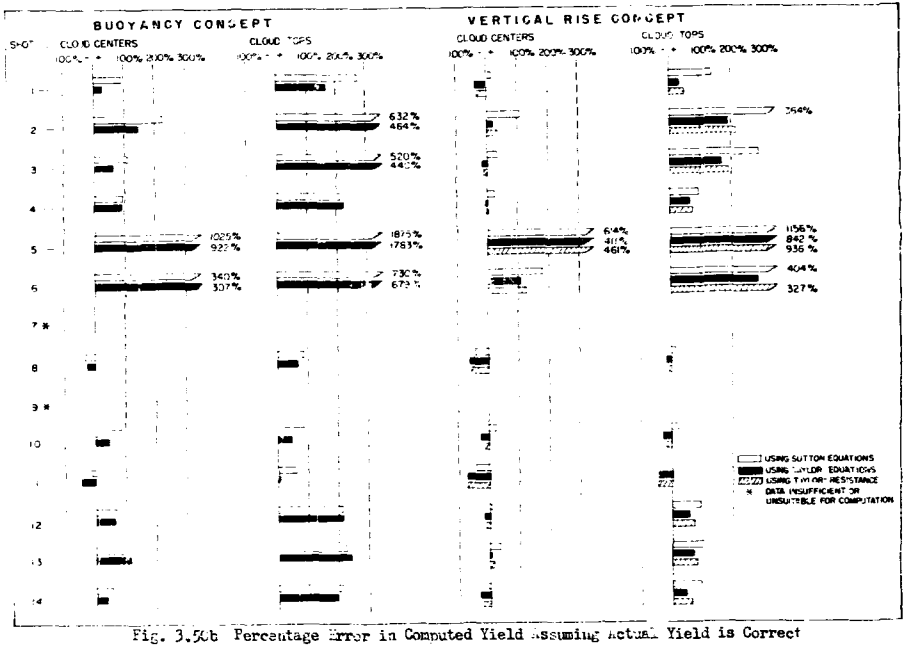

Fig. 3.50b Percentage Error in Computed Yield Assuming Actual Yield is Correct

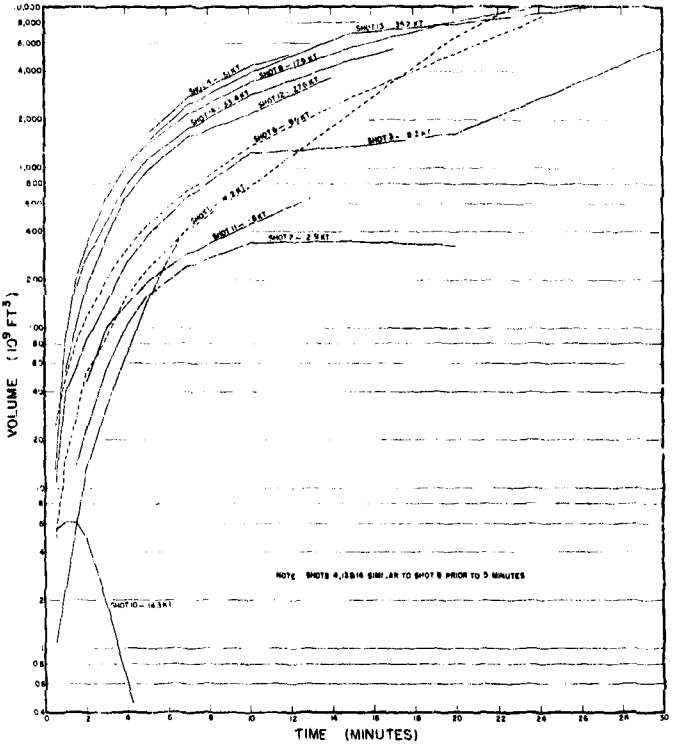

Fig. 3.51 Computed Cloud Volume vs Time

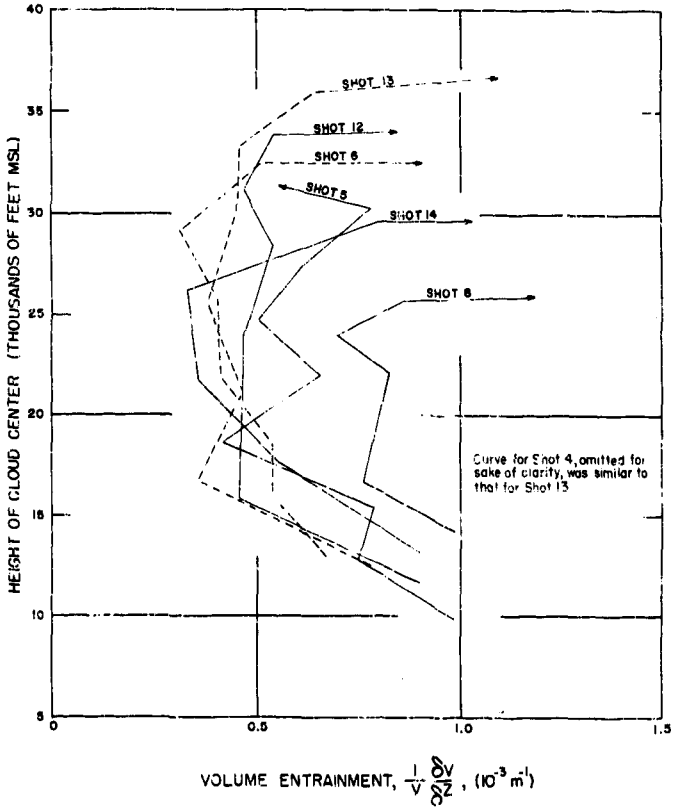

Fig. 3.52 Volume Entrainment vs Height of Cloud Center

CHAPTER 4

CONCLUSIONS AND RECOMMENDATIONS

4.1 CONCLUSIONS

The limitations of theodolite measurements were again quite clear. The experience on the TEAPOT series adds further proof to the dubious accuracy of theodolite data for earlier test series. In particular, readings after 8-10 minutes should be carefully examined for validity. According to EG&G photographic analysis of some of the bursts, the wind drift correction, as compared to photogrammetric triangulation methods, does not appear completely valid. In general the wind data smooth out directions and magnify the distances.

Cloud base data can be relied upon only with extreme caution. All methods of observation used have an inherent subjective bias in the determination of the actual base of the mushroom cloud. A sharp line of demarcation is usually not discernible due to various reasons, e.g., obstructing clouds, lack of proper lighting contrast due to shot time, irregular cloud features and layer formations in the stem portion of the cloud due to wind shears, gradual transition from mushroom to stem, etc. In general, it is reasonable to assume that most cloud base reports are at best a compromise.

The application of actual TEAPOT data to the current ideas about vertical cloud growth leaves much to be desired. The displacement of cloud centers, rather than cloud tops, produced somewhat better results when dynamic theory is applied but the necessity for further refinement is quite clear. More reliable heights for cloud bases, which in conjunction with heights of cloud tops determine the height of cloud centers used in the equations, might enhance the reliability of the dynamic approach. The use of these equations to determine yield from observed cloud rise also falls short of the desired accuracy.

The regression equation requires a redetermination of its constants in the light of more recent data which are considered more reliable. The introduction of other atmospheric parameters, e.g., moisture advection through entrainment, might result in some further improvement. The use of departures from the mean for terms like tropopause height, lapse rates, and mean wind in an actual sounding, may be a better measure of the atmosphere's role in determining cloud growth and development.

The use of a fixed maximum rise for all yields falling within a given range does not seem justified in the light of the data from this series.

Perhaps one of the most interesting bursts of the series was the high altitude shot. The height attained by that cloud did not conform the forecast height. In comparison with the usual stability of the stratosphere, the presence of relatively unstable conditions between 40,000 and 52,000 ft at shot time may also have contributed to the error in the forecast height. Paradoxically, the near absence of moisture in the stratosphere should have restricted the apparent size of the cloud and therefore its apparent rise. The former was verified by cloud volume computations, which show a decrease in the apparent volume after 0.5 minutes; however, the latter seems to have produced the reverse effect.

The most evident meteorological effect on cloud evolution noticed during this series was the dampening influence of the tropopause on cloud rise. Generally, attempts to correlate meteorological parameters with cloud height were non-conclusive.

This test proved that photogrammetric methods cannot be used for volumetric determinations on high altitude or prelaun shots. Due to field difficulties encountered on Shot 12, the feasibility of using photogrammetric methods on daytime tower shots was not determined. The dominant factor in the failure of the test was the non-synchronization of the camera due to radio signal failure. This precluded determining the effect of the following factors on the test: (1) Asymmetrical shape of cloud, (2) effect of rapid drift rate, at top of cloud, upon instrument projection distances, and (3) variations in density in different parts of the cloud. Portions of the cloud are of low density and contouring would probably not be possible.

SAC above-burst cloud photos were only of qualitative use because of complexity of geometry.

4.2 RECOMMENDATIONS

It appears that further study on existing and future cloud data is necessary to clarify the dynamics of cloud evolution.

Additional field operations and preliminary office study, are required to prove the feasibility of volumetric determination by photogrammetric compilation.

The preliminary office study should include improvement of the basic plan used on this test and investigation of possible major changes in procedure. Items to be studied: (1) Improvement of synchronization, (2) use of convergent photography, (3) use of photo theodolites, (4) area of cloud that may be compiled from one model, (5) length of camera base, (6) use of camera targets, (7) orientation of camera axis relative to drift direction, (8) number of cameras and bases to be used, (9) use of focal lengths of other than 6 inch, (10) camera station locations, and (11) effect of safety regulations on test procedure.

REFERENCES

1. P. Humphrey; Classified Scientific Meteorological Information (SANDSTONE); 1949 (Secret).
2. G. Kent, B. Holzman; Atmospheric Conditions and their Effects on Atomic Clouds at Nevada Proving Grounds (RANGER), WT-[illegible]; Jan. 1952 (Secret)
3. W. Kellogg, R. McKown, D. McPherson; The Development of the Atomic Cloud, Proj. 4.1b (GREENHOUSE); September 1951 (Secret).
4. E. Karstens: Air Weather Service Participation in Op. UPSHOT, WT-342; 31 December 1951 (Secret)
5. C. A. Spohn; Activities of the Special Weather Advisory Service (TUMBLER-SNAPPER) WT-552; November 1952 (Secret).
6. G. Newgarden; Activities of the Special Weather Advisory Service (UPSHOT-KNOTHOLE) WT-705; July 1953 (Secret).
7. EG&G; UPSHOT-KNOTHOLE Cloud Height and Drift Calculations, Report No. 1135; 6 April 1954 (Secret).
8. EG&G; Cloud and Stem Phenomena, Op IVY Report No. 1.36; 23 April 1954 (Secret).
9. EG&G; Technical Photography (IVY) WT-639; July 1954 (Secret).
10. L. Fussell; Cloud Photography, Proj. 9.1 (CASTLE, WT-933 May 1954 (Secret).
11. L. Machta; Entrainment and the Maximum Height of an Atomic Cloud, Bulletin of the American Meteorological Society; June 1951.
12. W. Kellogg - Rand Corp; The Rise of an Atomic Cloud from a Low Yield Device Detonated in the Stratosphere RM-1252; 19 March 1954 (Secret).
13. L. Gates, et al; The Residual Radiological Hazard from the Air Detonation of an Atomic Weapon in the Rain, NPSMP 201, p. 15, May 1953 (Secret).
14. S. Greenfield, et al, Rand Corp; Project Aureole, R-265-AEC; 1 July 1954 (Secret).
15. Edited by B. Grossman; Conference: Weather Effects on Nuclear Detonations, Air Force Surveys in Geophysics No. 31; Feb 1953 (Secret).
16. O. G. Sutton; Note on "Entrainment and the Maximum Height of an Atomic Cloud" by Lester Machta; Bulletin of the American Meteorological Society; June 1950.
17. G. I. Taylor, MDDC-919, 1945 (see Ref. 19).
18. O. G. Sutton, Weather 2 105, 1947.
19. R. A. Siddons: The Rise of the Cloud Produced by an Atomic Explosion, FWE-29; 12 November 1954 (Secret Restricted Data).
20. Cohen, Report B-15, 1945 (see Ref. 19).
21. W. Kellogg; The Height and Size of Atomic Clouds, RM-1378; 30 November 16, 1954 (Secret, Restricted Data).

[redacted]